



Profiling The Phytochemicals and Anti-SARS CoV-2 activity of Different *Ligustrum ovalifolium* Hassk Aerial Part Extracts: An *in vitro-in silico* Study



Ahmed H. Afifi^{1*}, Mohamed M. Ayoub¹, Omnia Kutkat^{2,3}, Mohamed GabAllah² and Reda S. Mohammed^{1*}
¹Pharmacognosy Department, Pharmaceutical and Drug Industries Research Institute, National Research Centre (ID: 60014618), 33 El Bohouth St., P.O. 12622, Cairo, Egypt
²Center of Scientific Excellence for Influenza Viruses, department of water pollution research division of environmental research and climate change. National Research Centre, El-Buhouth Street, Dokki, Cairo, 12622, Egypt
³Department of microbiology, Faculty of pharmacy, Ahram Canadian University, 6th of October, Giza 12566, Egypt

Abstract

Background: *Ligustrum* genus is part of the Oleaceae family it is commonly utilized as attractive trees or hedges in parks and gardens; it was most commonly seen in urban areas. *Ligustrum* species were broadly used in folkloric medicine. In China the plant was utilized to treat many illnesses, as rheumatic pains, cloudy vision, tinnitus, backache, sleeplessness, palpitations, and menopausal issues. Additionally, it was used to relieve symptoms associated with aging & as anticancer, antidiabetic, and hepatoprotective. *Ligustrum ovalifolium* (LO) Hassk was widely distributed in East Asia and is usually cultivated as an ornamental plant in many other countries. Methodology: The dried aerial non flowering parts of LO were extracted with MeOH (crude extract), part of crude extract was fractionated by liquid/liquid extraction with ethyl acetate (EtOAc) followed by n-butanol (n-BuOH), then the dried EtOAc fraction is partitioned between n-hexane and 90% methanol to obtain five different fractions which were *in vitro* screened against SARS-CoV-2. Results: All extract fractions had high safety on Vero-E6 cells and exhibited activity against SARS-CoV-2. The highest activity was attributed to the 90% methanol fraction with (IC₅₀) = 7.895 µg/ml and safety index (SI) = CC₅₀/IC₅₀ = 5851/7.895 = 741.1. Analysis of the active fraction (90% methanol) using LC-MS/MS resulting in the detection of 77 metabolites in negative ionization modes. They were arranged according to their abundant as: iridoid, phenylethanoid and phenylpropanoid compounds, triterpenoids, lignans, flavonoids, phenolic acids, long chain fatty acids and coumarin. Molecular docking study was used to investigate the binding affinity of the detected compounds against SARS Cov-2 main protease (M^{Pro}) and spike protein (S). It was found that acteoside (25), (2''R)-10-hydroxy-2''-methoxyoleuropeins (31), ligustaloid A (34) and rutin (19) exhibited outstanding binding affinities toward the active site of M^{Pro} and achieved docking scores of -13.58, -11.93, -11.92 and -11.22 kcal/mol, respectively. On the other hand, the best binding affinities against receptor binding domain (RBD) of SARS Cov-2 spike protein were exhibited by ligupurpuroside A (33), isoacteoside (29), ibotalactone B (14) and acteoside (25) they have achieved docking scores of -10.16, -8.97, -8.43 and -7.97 kcal/mol respectively. Conclusion: *L. ovalifolium* Hassk 90% methanol fraction enriched with valuable compounds as iridoids, phenylethanoid/propanoids & triterpenoid derivatives of oleanolic acid & ursolic acid these compounds were responsible for the antiviral activity against SARS-Cov2. This is the first study done on *L. ovalifolium* Hassk aerial parts which revealed the detection compounds via LC/MS/MS. Additionally, the screening of the *in vitro* & *in silico* antiviral activity against SARS CoV-2 were first evaluated in this study.

Keywords :*Ligustrum ovalifolium*, SARS Cov-2, LC/MS/MS, iridoid, phenylethanoid and phenylpropanoid, triterpenoids

1. Introduction:

Oleaceae family include important plants of economic values: as the olive tree and *Ligustrum* (privets) [1]. Plants of this family are distributed throughout the world, they are especially abundant in tropical and temperate Asia. The tropical and warm-temperate species are evergreen; those from the colder north temperate zone are deciduous. Iridoids and phenylethanoid derivatives in the form of esters and glycosides of tyrosol and hydroxytyrosol are characteristic compounds of Oleaceae plants. In the genus *Ligustrum* most of the identified iridoids formally belong to secoiridoids, as well as oleoside-type glycosides [2]. The *Ligustrum* genus, which belongs to the Oleaceae family, has around 20 species, subspecies, and variants. These trees are mostly found in urban areas and are commonly employed as decorative hedges or trees in parks and

*Corresponding author e-mail: a_afifi1979@hotmail.com (A. Afifi), redamohammed2015@gmail.com (R Mohammed)

Received date: 09 June 2024; Revised Date: 20 July 2024; Accepted date : 21 July 2024

DOI: 10.21608/EJCHEM.2024.296342.9836

©2025 National Information and Documentation Center (NIDOC)

gardens[3]. *Ligustrum* species are broadly used in folkloric medicine, their traditional usage is approved as; anti-inflammatory, antidiabetic, antioxidant and pro-apoptotic[4,5]. Previous studies on *Ligustrum* species have shown notable pharmacological properties as antioxidants, hepatoprotective, neuroprotective, and anti-mutagenic[6-8]. *Ligustrum(L)* is enriched with important phytoconstituents as secoiridoids, phenylethanoids, flavonoids and triterpenes which were reported to have various biological activities [9-13]. *L. japonicum* Thunb. distributed in Japan and Korea was reported for its secoiridoid compounds detected in the leaves and fruits and triterpenoids as ursolic acid, oleanolic acid, which were isolated from the *L. japonicum* pericarp[14]. *L. lucidum* Ait. fruit is one of medicinal herbs officially approved by the Ministry of Health of P.R. China as a dietary supplement[15]. In China, *L. lucidum* Ait is frequently used for menopausal symptoms, rheumatic pains, impaired vision, tinnitus, palpitations, backaches, sleeplessness, and age-related ailments. It also has antidiabetic, hepatoprotective, and anticancer properties [16,5&17]. Flavonoids, secoiridoids, triterpenes, and polysaccharides are some of the chemical components of *L. lucidum* Ait. fruit that may be responsible for its pharmacological effects.[18,13,19]. The most important is its use in combination of many herbal formula in clinical practice to strengthen bones, for the treatment of osteoporosis *via* promoting osteoblast cell mineralization, preserving calcium homeostasis, and raising blood parathyroid hormone levels [20-23]. *Ligustrum ovalifolium* Hassk is the plant of our study, it is widely distributed in East Asia and is usually cultivated as an ornamental plant in many other countries[24]. The plant is enriched with important constituents as acylated triterpenoids from flowers[25], and secoiridoid glucosides with hypotensive activities from leaves[26].

To our knowledge there is no complete phytochemical characterization performed on *Ligustrum ovalifolium* Hassk aerial parts so the present study was designed to investigate the *in vitro* activity of different extract of *L. ovalifolium* aerial parts on SARS CoV-2 virus. The contents of the active extract were analyzed through HPLC-MS/MS, some of the identified compounds were screened for *in silico* molecular docking study in an attempt to discover natural extracts enriched with bioactive compounds with activity against SARS CoV-2 virus.

2. Material and methods

2.1. Plant material

The *L. ovalifolium* non flowering aerial parts were collected during spring from Zoological Garden 2022, Giza, Egypt, the plant was kindly identified by Mrs. Terasa Labib, plant taxonomist of Al-Orman Garden.

2.2. Preparation of the extract

The dried aerial parts of *L. ovalifolium* (250 g) were powdered and extracted with methanol (MeOH) (1L x 3) till exhaustion. The combined methanolic extract was dried under reduced pressure in a rotary evaporator at 40C to yield 40 gm of dried crude extract (fraction 1). 40 gm of the crude extract was suspended in water (200 ml) transferred to separating funnel and subjected to liquid /liquid extraction with ethyl acetate (EtOAc) followed by butanol (n-BuOH fraction 4) till exhaustion, the remaining aqueous solution left was dried under vacuum to give aqueous fraction 5.

The dried EtOAc-soluble extract (15 g) was then partitioned between n-hexane (fraction 2) and 90% methanol (fraction 3) to yield 2.5 & 12 gm respectively(Fig1). All solvent used are of analytical grade from Adwic (Egypt)

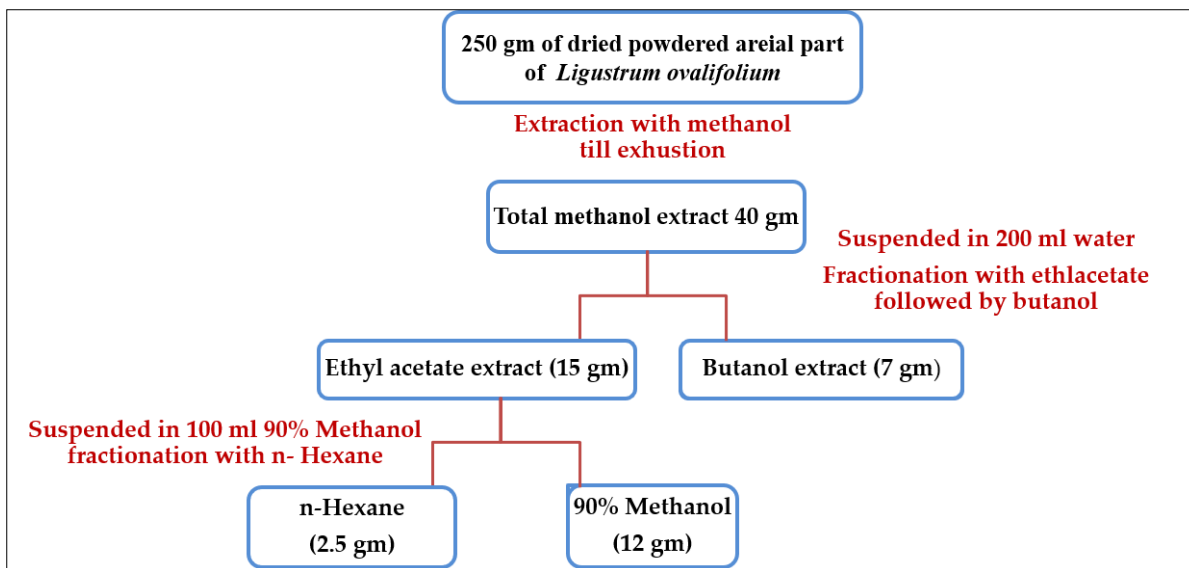


Figure 1: Schematic diagram of extraction of the aerial parts of *L. ovalifolium* Hassk

3. Biological study

3.1. MTT cytotoxicity assay

For determination of the half maximal cytotoxic concentration (CC_{50}). Stock solutions of the test compounds were prepared in 10 % DMSO in ddH₂O and diluted further to the working solutions. The extracts were tested on African green monkey kidney VERO-E6 cells (ATCC No. CRL-1586) which were grown in (Dulbecco's modified Eagle's medium; DMEM Gibco, Waltham, MA, USA) with 4% Fetal Bovine Serum (FBS Gibco, Waltham, MA, USA) and 2% from antibiotic antimycotic (Gibco). The cytotoxic activity of the extracts was tested in by using the 3-(4, 5-dimethylthiazol -2-yl)-2, 5-diphenyltetrazolium bromide (MTT) (Sigma-Aldrich, USA) method was performed as described by Rawah et al 2023[27]. Absorbance of formazan solutions was measured at λ max 540 nm with 620 nm as a reference wavelength using a multi-well plate reader. The following formula was used to calculate the percentage of cytotoxicity relative to untreated cells. The concentration that demonstrated 50% cytotoxicity (CC_{50}) was found using a plot of percentage cytotoxicity against sample concentration.

$$\% \text{ cytotoxicity} = \frac{(\text{absorbance of cells without treatment} - \text{absorbance of cells with treatment})}{(\text{absorbance of cells without treatment})} \times 100$$

3.2. Inhibitory concentration 50 (IC_{50}) determination

In 96-well tissue culture plates, 2.4×10^4 Vero-E6 cells were distributed in each well and incubated overnight at a humidified 37°C incubator under 5% CO₂ condition. The cell monolayers were then washed once with 1x PBS balanced salt solution was prepared in lab (genomix laboratories) and subjected to virus adsorption (hCoV-19/Egypt/NRC-03/2020 (Accession Number on GSAID: EPI_ISL_430820)) for 1 h at room temperature (RT). The procedure was preceded as reported Rawah et al 2023[27]. The optical density of the color is measured at 570 nm using Anthos Zenyth 200rt plate reader (Anthos Labtec Instruments, Heerhugowaard, Netherlands). The IC_{50} of the compound is that required to reduce the virus-induced cytopathic effect (CPE) by 50%, relative to the virus control[28].

2.4. Phytochemical study

2.4.1. LC/MS/MS

Instrument: Liquid chromatography-electrospray ionization-tandem mass spectrometry (LC-ESI-MS/MS) was used to analyze the material. An Exion LC AC system was used for separation, and a SCIEX Triple Quad 5500+ MS/MS system with an electrospray ionization (ESI) detector was used for detection. The separation was accomplished with a Ascentis® Express 90 Å C18 Column (2.1×150 mm, 2.7 µm). The mobile phases were consisted of two eluents A: 5 mM ammonium formate pH 8; B: acetonitrile (LC grade), and the gradient elution conditions were: 5% B from 0-1 min, 5-100% B from 1-21 min, 100% B from 21-25 min, 5% B from 25.01-30 min. flow rate was 0.3 ml/min and the injection volume was 5 µl. For MS/MS analysis, negative ionization mode was applied with a scan (EMS-IDA-EPI) from 100 to 1000 Da for MS1 with the following parameters: curtain gas: 25 psi; IonSpray voltage: -4500; source temperature: 500°C; ion source gas 1 & 2 were 45 psi and from 50 to 1000 Da for MS2 with a declustering potential: -80; collision energy: -35; collision energy spread: 15.

2.5. In silico studies

2.5.1. Preparation of ligands

The 3D structures of the identified phytoconstituents were either obtained through 2D sketching using ChemBioDraw Ultra 14.0 followed by generation of 3D structure using Chem 3D Pro 14.0 or by direct download of the 3D structure from PubChem chemical database (<https://pubchem.ncbi.nlm.nih.gov/>) in .sdf format. All structures were energy minimized using MMFF94 force field and saved in .pdbqt format after gasteiger charges were assigned for each structure

2.5.2. Preparation of target proteins

The co-crystal structures of SARS Cov-2 Main protease (M^{Pro}) in complex with non-covalent inhibitor, 5-(3-{3-chloro-5-[(2-chlorophenyl) methoxy]-4-fluorophenyl}-2-oxo-2H-[1,3'-bipyridin]-5-yl) pyrimidine-2,4(1H,3H)-dione (PDB:7M8P) and spike receptor binding domain (RBD) bound to human ACE2 (PDB:6M0J) were downloaded from RCSB PDB (www.rcsb.org). Crystal structures were prepared by removal of all water molecules, ions and other HET atoms followed by addition of hydrogen atoms, missing atoms and residues. Correct protonation and tautomerization states of histidine, glutamic, aspartic, lysin and cysteine were adjusted and finally energy minimization with steepest descent protocol with 100 steps and 0.02 step size along with conjugate gradient with 10 steps and step size 0.02 Å was applied. Prepared structures were saved in .pdbqt format after assignment of partial charges for docking process.

2.5.3. Molecular docking

Molecular docking of identified phytoconstituents with M^{Pro} and spike RBD was achieved using AutoDock vina by PyRx 0.8 version. Grid boxes with dimensions of 60X60X60 points and grid point spacing of 0.375 Å was generated to specify the binding pocket of both target proteins. For M^{Pro} the grid box was centered on the co-crystallized ligand while for spike RBD it was centered on the residues Gly446, Tyr449, Tyr453, Leu455, Ala475, Glu484, Phe486, Asn487, Tyr489, Gln493, Ser494, Gly496, Gln498, Asn501 and Tyr505 which were reported to play crucial rule in the binding of spike RBD to hACE2.[29] The docking poses were ranked according to their binding energies and best poses were visualized and analyzed using Discovery Studio Visualizer 2020[30].

3. Results & discussion

3.1. Biological activity

The five different fractions of *L. ovalifolium* Hassk aerial parts were tested against SARS-CoV-2. All fractions exhibited antiviral activity against SARS-CoV-2 and great advantage, they had high safety on Vero-E6 cells so they are safe to normal cells and can be used on cells with high concentrations. The highest activity is attributed to 90% methanol fraction with inhibitory concentration (IC₅₀) = 7.895 µg/ml and safety index(SI) = CC₅₀/IC₅₀ = 5851/7.895 = 741.1. followed by hexane

fraction (2) with SI= 335.9, crude extract (1) with SI = 219.19 & the lowest is the aqueous fraction (5) with SI = 92.3.

On other hand the n-BuOH fraction (4) had no antiviral activity against SARS-CoV-2(Fig.2).

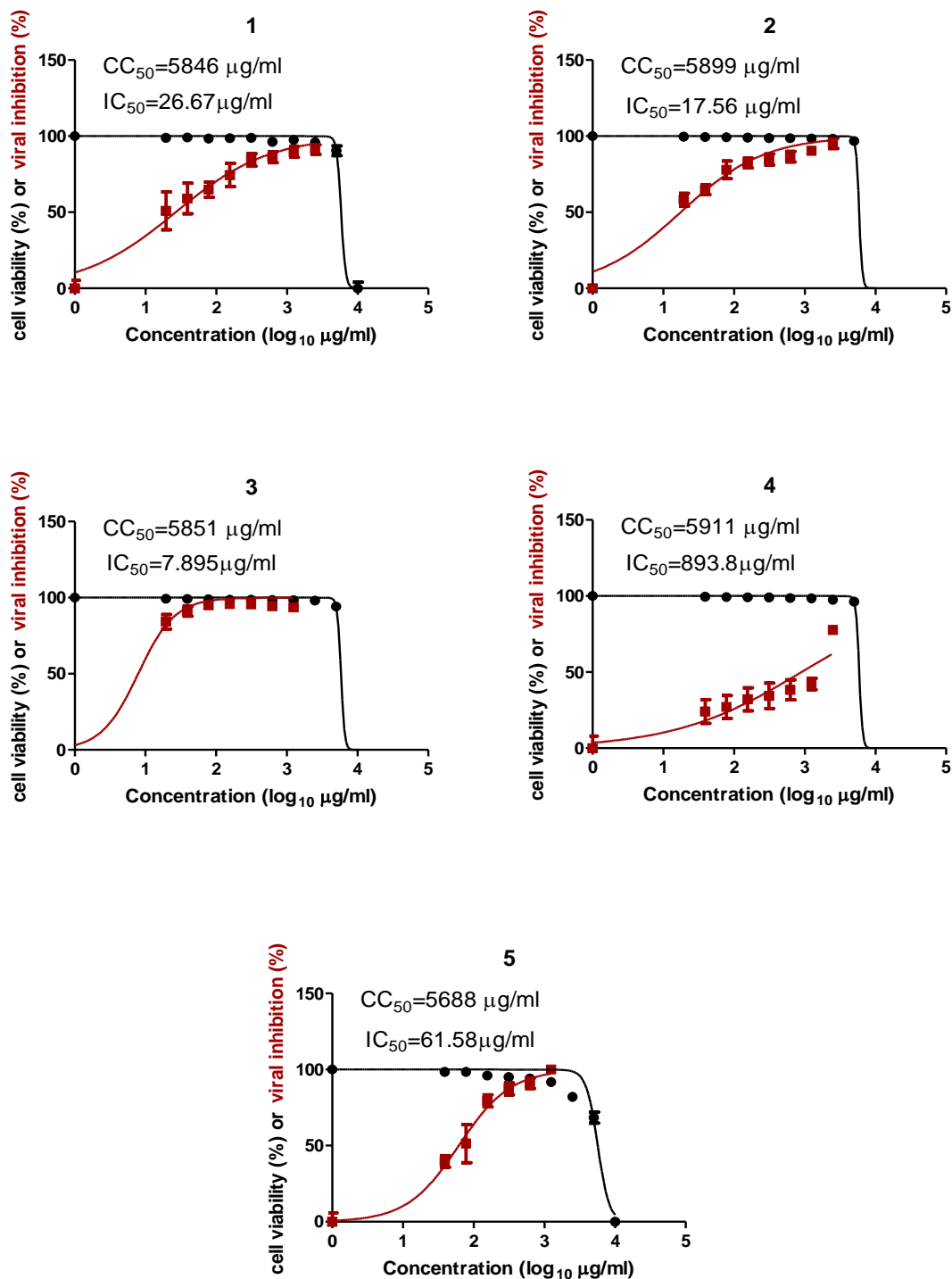


Fig 2. Graph of Cytotoxicity concentration 50 (CC₅₀) and Inhibitory concentration 50(IC₅₀) Crude extract (1) hexane fraction (2) ETOAc extract (3) n-BuOH fraction (4) & aqueous fraction(5)

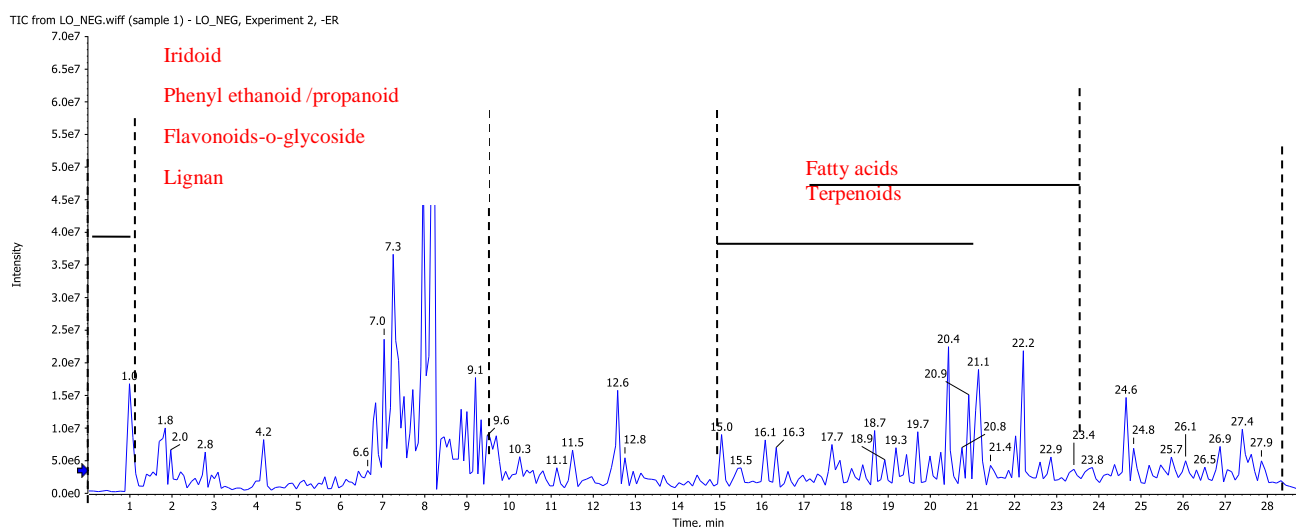


Fig. 3: ESI-MS chromatogram of *L. ovalifolium* in negative ionization mode

3.2. Phytochemical study

3.2.1. HPLC profiling and MS analysis

L. ovalifolium, belongs to the olive family Oleaceae [31, 24] This family is characterized by large number of bioactive constituents mainly monoterpenoids, iridoids, secoiridoids, phenylethyl alcohols and flavonoids[32]. LC-MS/MS analysis was used to examine the 90% physiologically active methanolic fraction of the aerial parts of *L. ovalifolium*. Metabolite elution occurred in a runtime of about 28 minutes, with metabolites eluted in order of polarity, from most polar to least polar. According to available literature data, they were identified using retention time (Rt), MS data (molecular ion, fragmentation pattern.), compared to reported literature data (MS databases (FooDB, HMDB and Massbank)[33,34]. Fig 3 represents the base peak chromatogram (BPC) of the detected metabolites in 90% methanol (fraction3) of *L. ovalifolium* Hassk. Some of the metabolites discovered had previously been reported in other *Ligustrum* species. LC-MS/MS analysis in negative ionization mode, 77 metabolites belonging to diverse chemical classes were identified (Table 1). Iridoids were the most abundant class, followed by triterpenoids, phenylethanoid/ phenylpropanoid compounds, lignans, flavonoids, phenolic acids, long-chain fatty acids, and coumarins. BPC of fraction 3 revealed that iridoids and triterpenoids, the most prevalent metabolites with a broad spectrum of biological activities, eluted between 2.57- and 21.8-minutes retention time (Rt).

Phenolic acids

In the negative ion mode, phenolic acids produced deprotonated [M-H]⁻ fragment ions, which in MS2 provide distinctive diagnostic fragments. resulting from either dehydration (-H₂O), decarboxylation (-COO⁻), demethylation (-CH₂) or demethoxylation -OCH₂, the following six phenolic acids and their derivatives were detected e.g. vanillic acid (1) *m/z*, 167.00 [M-H]⁻ C₈H₈O₄⁻ [34]; chlorogenic acid (2) *m/z*, 352.96 [M-H]⁻, (C₁₆H₁₇O₉)⁻ [35], caffeic acid (8) *m/z*, 179.03 [M-H]⁻, C₉H₈O₄⁻ [36]; ferulic acid (50) *m/z* 193.02 [M-H]⁻, C₁₀H₁₀O₄⁻; feruloyl quinic acid (5) and coumaroyl quinic acid (10) *m/z*, 367.00 [M-H]⁻, C₁₇H₁₉O₉⁻ & *m/z*337.02[M-H]⁻ C₁₆H₁₇O₈⁻ as the fragments 191 correspond to [quinic aid -H]⁻ [37].

Flavonoids

Flavonoids break within the aglycone, producing small neutral molecules and fragments. through the Retro-Diels–Alder (RDA) reaction e.g., CO, CO₂ and H₂O [38]. Nine different flavonol & flavone glucosides or their aglycones were

characterized in the studied extract (quercetin, kaempferol, apigenin & luteolin). Two quercetin derivatives were detected in accordance with an *O*-glycosidic cleavage: quercetin -*O*-hexoside (15) m/z 462.93 [M-H]⁻ C₂₁H₁₉O₁₂⁻, and rutin (19) [M-H]⁻ 609.92 (C₁₇H₂₉O₁₆)⁻ [39]. Two kaempferol derivatives: kaempferol-*O*-hexoside (26) m/z 446.95, [M-H]⁻, (C₂₁H₁₉O₁₁)⁻, and kaempferol-*O*-methyl ether (64) m/z 299, C₁₆H₁₁O₆⁻, the daughter ions at m/z 284[M-H-CH₃]⁻. indicate the methoxylated flavonoid [40,41]. Four apigenin derivatives: rhoifolin (35, apigenin 7-*O*-neohesperidoside) m/z 577.02, [M-H]⁻ C₂₇H₂₉O₁₄⁻, apigenin 7-*O*-hexoside (40), m/z 431.00[M-H]⁻, C₂₁H₁₉O₁₀⁻; isorhoifolin (41) (apigenin-7-*O*-rutinoside) m/z 577.00 [M-H]⁻ C₂₇H₂₉O₁₄⁻; and apigenin (62) m/z 269.03, C₁₅H₉O₅⁻. Luteolin aglycone was also detected (49) m/z 285.00, C₁₅H₉O₆⁻. It was reported that apigenin derivatives were previously detected in *L. lucidum* Ait leaves [42].

Phenylethanoid derivatives (Tyrosol derivatives)

Ligustrum species characterized by presence of phenylethanoid & phenylpropanoid compounds [43,44](Fig 3A). They undergo fragmentation pathway to give neutral fragments as dehydration -H₂O, glycosidic cleavage [-162 hexosyl, -146 rhamnosyl], -OCH₂ loss of methoxy group[42]. In our study five phenylethanoid compounds were detected as; hydroxytyrosol glucoside (3) with [M - H]⁻ at m/z 315.00, C₁₄H₁₉O₈⁻; hydroxytyrosol (4) m/z 153.02, C₈H₉O₃⁻; tyrosol (7) m/z 137.00, C₈H₉O₂⁻, salidroside (8) m/z , 299.01, C₁₄H₁₉O₇⁻, and ibotanolid B (27), m/z 477.00, C₂₃H₂₅O₁₁⁻. Compounds (3, 8 & 27) were glycoside derivatives of tyrosol with ibotanolid B acylated with caffeic acid at OH no 6 of the glucose. These compounds showed their characteristic fragments at m/z , 137[M-H-162 (glucosyl)]⁻, 179 [glucose-H] 119 [M-H-180 (glucose)]⁻ & the fragments 315[M-H]⁻ - caffeoyl], 179[caffeic acid -H], 161[caffeic acid-H-H₂O]. The two fragments 137 and 315 correspond to tyrosol and hydroxyl tyrosol glucoside respectively [45,46].

Phenylpropanoid compounds

Three phenylpropanoid compounds with two or three sugar residues were detected and identified as acteoside and its isomers isoacteoside (25&29) m/z 622.98[M-H]⁻, C₂₉H₃₅O₁₅⁻ and ligupurpurosides A (33) with m/z 769.00, (C₃₅H₄₅O₁₉)⁻ with characteristic fragmentation as: [M- H- caffeoyl]⁻, [M-H- caffeoyl-(glucosyl-rhamnosyl)]⁻ or [M-H-caffeoyl-2rhamnosyl]⁻; the fragment m/z 161 corresponds to[caffeic-H-H₂O]⁻ [47, 48, 39,49]. Acteoside and its isomers isoacteoside showed various pharmacological activities, including antioxidant, anti-inflammatory, in addition to other health benefits[50].

Iridoids compounds

Iridoids are highly oxygenated monoterpenes. These substances are widely distributed across the angiosperm plants as secondary plant metabolites. Their structure is cyclopentanopyran form, cleavage of cyclopentane ring at C-7-C-8 gives rise to a subclass known as secoiridoids[51].(Fig.3 B). Iridoids which have hemiacetal hydroxyl groups are active in nature, they are mostly occur in the form of glycosides at the C-1 hydroxyl group[52,53]. They are more prevalent in the dicotyledon plants including Oleaceae family [54, 55]. Many biological effects such as liver protection, anti-inflammatory and anti-tumor effects were reported for iridoid compounds [56, 57, 58]. This study revealed the detection of 29 iridoids in the negative ionization mode, they are found mostly as glycoside or acetylated derivatives (Fig 3B, 3C&3D), where the MS2 undergo glycosidic and ester bonds breakage then ring-opening reaction of the iridoid parent ring. This process produced various characteristic fragments with relative abundance, which could accurately characterize the structures of various parts of the compounds.[39]. In our study LC/MS of *L. ovalifolium* Hassk aerial parts in the negative mode revealed identification of large number of secoiridoid compounds which behave similar in MS/MS fragmentation as [M-H]⁻ and [M-H-(glucosidic cleavage (-glucose /rhamnose))]⁻. For the acylated derivative (6, 11&12) with caffeic acid the fragments [M-H-(162 caffeoyl)]⁻, 179[caffeic -H]⁻, 161[caffeic -H-H₂O]⁻ were detected[59].

Secoiridoids

Ligujaponoside A(21) m/z 555.00 [M-H]⁻, C₂₅H₃₁O₁₄⁻ and its hydroxyl derivative ligujaponoside B(18) m/z 571.01 [M-H]⁻

C₂₅H₃₁O₁₅⁻ they belong to secoiridoid and characterized by presence of COOCH₃ group at position 4 and sugar at position 1 of the pyran ring in iridoid structure it behave in LC/MS as [M-H-MeOH], [M-H- MeOH-hexosyl-H₂O] & 179 [Hexose – H]⁻ [14]. Four ligustaloside secoiridoid derivatives were detected: Ligustaloside A (34) with [M-H]⁻ m/z 554.94, C₂₅H₃₁O₁₄⁻; Ligustaloside B (44) m/z 539.03, C₂₅H₃₁O₁₃⁻; ligustaloside A dimethyl acetal (53), m/z 601.01, C₂₇H₃₇O₁₅⁻; and ligustaloside B dimethyl acetal, (58) m/z , 585.05, C₂₇H₃₇O₁₄⁻ their fragmentation as compounds 18 & 21 and as reported [59,39].

Additionally, Ligustroside (59) m/z 523.17 [M-H]⁻, C₂₅H₃₁O₁₂⁻, ligustrohemiactal B (48) m/z 377.03 [M-H]⁻, C₁₉H₂₁O₈⁻ and liguluciridoids B, (69) m/z 301.14 [M-H]⁻, C₁₄H₂₁O₇⁻ were also detected [60,61].

Three isomers nuezhenide, isonuezhenide, specnuezhenide (isomer of nuezhenide) & neonuezhenide which is hydroxyl derivative of nuezhenide (32, 43, 36 & 24) with m/z 685 [M-H]⁻, C₃₁H₄₁O₁₇⁻ & m/z 701.01 [M-H]⁻, C₃₁H₄₁O₁₈⁻, respectively with MS2 fragments m/z 523 /or 539 [M-H- glucosyl]⁻, bond cleavage occurred at carbon 2 /oxygen 1 and carbon 5/ 9 to produce m/z 453/or 463 [M-H-glucosyl-C₄H₆O]⁻, other fragments results from breakage of ester group m/z 523, 223, 299 & m/z 315 [the latter two fragments are tyrosol glucoside & hydroxytyrosol glucoside moiety respectively] [62,39,63]

Nuzhenal A: (30), it is considered the non-glycosidic secoiridoid with m/z [M-H]⁻, 213.12, C₁₀H₁₃O₅⁻, with MS2 fragments at m/z 183 [M-H-CH₂O]⁻, 195 [M-H-H₂O]⁻, 177 [M-H-2H₂O]⁻ [63, 19]. Four Lucidumoside A, B, C & D (60, 52, 61 & 46) are detected with [M-H]⁻ m/z 525.03, C₂₅H₃₃O₁₂⁻; m/z 541.01, C₂₅H₃₃O₁₃⁻; m/z 583.02, C₂₇H₃₅O₁₄⁻, & m/z 567.02, C₂₇H₃₅O₁₃⁻. The obtained mass data of these compounds matched the reported data, confirming their identity, they were previously isolated from *L. lucidum* [10, 64].

Four secologanosides: caffeoyl secologanoside (6) m/z 550.95 [M-H]⁻, C₂₅H₂₇O₁₄; coumaroyl secologanoside (11) m/z 535.00, C₂₅H₂₇O₁₃⁻ and feruloyl secologanoside (12), m/z 565.00, C₂₆H₂₉O₁₄⁻ & secologanin (65) m/z 387.04 [M-H]⁻, C₁₇H₂₃O₁₀⁻. In the first three compounds the sugar is acylated with either caffeic, coumaric or ferulic acid therefore they undergo fragmentation in MS2 as [M-H-CO₂]⁻, [M-H-162 caffeoyl /or 146 coumaroyl /or 176 feruloyl], 179 [caffeic acid-H], 161 [caffeic acid-H-H₂O] / [coumaric acid-H], [coumaric acid-H-H₂O], [ferulic-H], [ferulic-H - H₂O] [M-H-C₁₀H₁₂O₆]⁻ [59,65].

Two lactone type secoiridoid with COOH group at position 4 of pyran ring were detected and identified as: ibotalactone A & B (hydroxyl derivative) (20 & 14), m/z 535.00, [M-H]⁻ C₂₅H₂₇O₁₃⁻ and 550.99 [M-H]⁻, C₂₅H₂₇O₁₄⁻ where the sugar moiety is acylated with coumaric or caffeic acid and they behave like compounds 6, 11 & 12 [66].

Hydroxyphenethyl -7-O-glucosideelenolic acid ester (39) is a secoiridoid ester with the glucosylation at carbon 7 with m/z [M-H]⁻, 523.00, C₂₅H₃₁O₁₂⁻ with characteristic MS2 in accordance with reported data [67].

Oleoside-type secoiridoids

Oleosides belong to secoiridoids, they are characteristic compounds for the Oleaceae family [64]. Oleoside and secologanoside had been reported in the genus *Ligustrum* [2]. In the current study eight oleoside derivatives were detected in *L. ovalifolium* Hassk aerial parts: they are; 10-Hydroxyoleoside dimethyl ester (17) m/z 433.00, C₁₈H₂₅O₁₂; methyl glucooleoside (22) 564.95, C₂₃H₃₃O₁₆⁻; 10-Hydroxyoleuropein (28) 555.00, C₂₅H₃₁O₁₄⁻; (2`R)-10-hydroxy-2`-methoxyoleuropeins (31) 585.00, C₂₆H₃₃O₁₅⁻; Oleuropeinic acid (51) 569.95, C₂₅H₂₉O₁₅⁻; Oleuropein (54) 539.01, C₂₅H₃₁O₁₃⁻; Oleurosides (55) 539.02, C₂₅H₃₁O₁₃⁻ and Oleoside-11- methyl ester (47) 403.04, C₁₇H₂₃O₁₁⁻. These compounds share similar MS2 fragments which include m/z [M-H-CH₃OH]⁻, [M-H- hexosyl]⁻, [M-H-hexose-CH₃OH]⁻, neutral loss of CO₂ and H₂O [68, 69]. In our study 29 secoiridoid compounds were identified, known for their diverse bioactivities. These isolated secoiridoids from *L. lucidum* fruit

exhibited antioxidant, antiosteoporosis, hypolipidemic, and antiviral activities[70]. The antiviral activity against the parainfluenza type 3 virus (Para 3) and the respiratory syncytial virus (RSV) was also reported for these compounds[71]. Oleuropein had significant activity against RSV and Para 3 with IC₅₀ values of 23.4 and 11.7 µg/mL respectively. Additionally, Lucidumoside C, Oleoside dimethyl ester and ligustroside displayed potent or moderate antiviral activities against Para 3 with IC₅₀ values of 15.6-20.8 µg/ml [71]. In the current study the active extract fraction 3 was enriched with the previously reported compounds this finding may explain the anti-SARS CoV-2 activity of the active 90% methanolic fraction (fraction 3).

Triterpenoids

Triterpenoids were an important class of compounds of the genus *Ligustrum*, the two isomers oleanolic (OA) and ursolic acid (UA), have strong hepatoprotective efficacy against acute liver damage caused by numerous agents as well as chronic liver fibrosis [17]. Three pentacyclic triterpenoid acids, two hydroxylated triterpenoid acids and one β- amyrin diol were detected in LO and identified as: betulinic acid, oleanolic acid, ursolic acid (72, 74,75) with *m/z* [M-H]⁻ 455.27, 455.22, 455.33, respectively and hydroxyoleanolic acid, hydroxyursolic acid (66 &67) with *m/z* [M-H]⁻ 471.18 & 471.20 and molecular ion C₃₀H₄₇O₃⁻, respectively. These compounds share similar MS² fragments explained by neutral loss of H₂O, CO₂, HCOOH it includes *m/z* 407 [M-H- HCHO-H₂O], 409 [M-H-HCOOH] [72,73], these compounds were previously reported in *L. lucidum*. [74-76].

Erythrodiol (76) *m/z* [M-H]⁻, 441.08, C₃₀H₄₉O₂⁻ is the detected pentacyclic triterpenoid diol it is derivative of β-amyryn with CH₂OH group at position 28, It is a plant metabolite found in olive oil, the deprotonated ion peak at MS² undergo fragmentation as reported [77]. Both OA and OA+UA have potential effect as antiosteoporosis [78]. They demonstrated hepatoprotective activity. A variety of pharmacological effects have been reported by the water extract of fruit *L. lucidum* as antiosteoporosis[79,59], antiviral activity,[80] antioxidant, hypoglycaemic [81] antitumor activity and other biological activities [82, 83].

Lignan Olivil derivatives

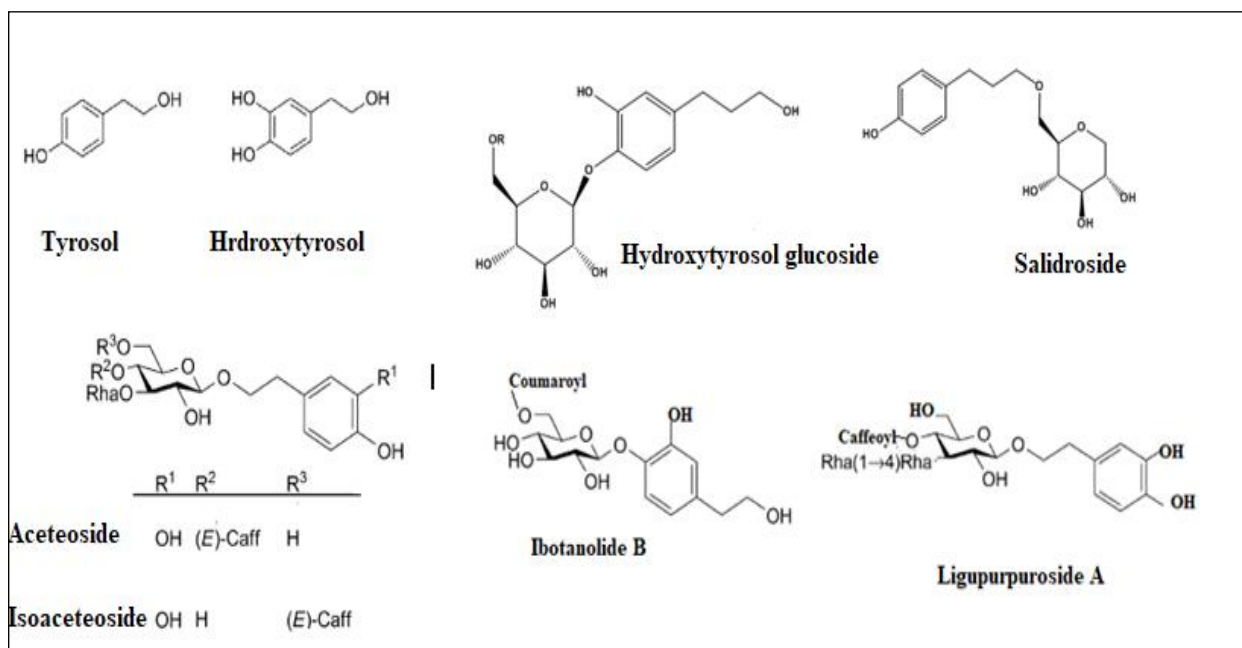
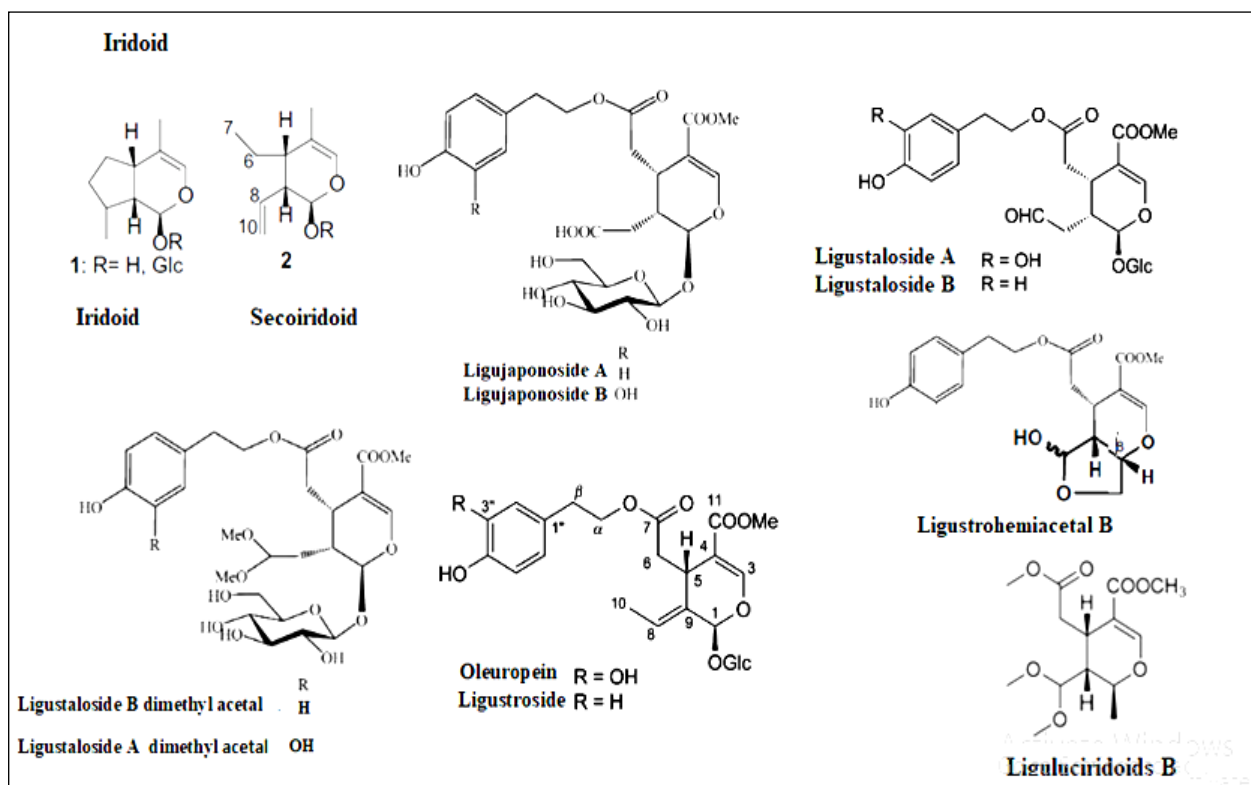
Olivil and its glycoside derivative belong to lignan compounds, the provided ion fragments in the LC/MS, consistent with the opening and cleavage of the tetrahydrofuran ring and further losses of CH₃ and H₂O, the glycoside derivatives undergo deglycosylation[84]. In our study six lignan compounds or their glycosides are detected as: olivil-*O*-glucoside (16) [M-H]⁻, *m/z* 537.00, C₂₆H₃₄O₁₂, olivil (23) *m/z* 375.01⁻, C₂₀H₂₄O₇⁻, Eucommin A (45), 549.09, C₂₇H₃₃O₁₂⁻, syringaresinol-*O*-glucoside, (56) *m/z* 579.01, C₂₈H₃₆O₁₃⁻ & pinoresinol-*O*-glucoside (37) 519.04, C₂₆H₃₂O₁₁⁻ and pinoresinol (42)*m/z*,357.02, C₂₀H₂₂O₆⁻. According to the fragment ions of these compounds, the fragment ions *m/z* 327, [C₁₈H₁₅O₆]⁻, *m/z* 357 [C₂₀H₂₁O₆]⁻, *m/z* 387 [C₂₁H₂₃O₇]⁻ or [C₂₀H₁₉O₈]⁻ containing the parent nucleus are the characteristic fragment ions of lignans nucleus [84,85]. Studies have shown that lignans are related to reducing the risk of cardiovascular disease [86]. Sesame seeds and olive oil contain pinoresinol, previous research has shown that pinoresinol controls a number of brain processes, such as memory and learning [87].

Fatty acids

Five straight chain fatty acids are detected as linolenic acid (68) 277.13, C₁₈H₂₉O₂, hexadecenoic acid (70) 253.14, C₁₆H₂₉O₂, hexadecanoic acid (71) *m/z* 255.16, C₁₆H₃₁O₂⁻, 255.16, linoleic acid, (73) *m/z* 279.16, C₁₈H₃₁O₂⁻ and oleic acid (77) *m/z* 281.16, C₁₈H₃₃O₂⁻.

Coumarin

Esculetin (13) *m/z* 177.00 [M-H]⁻, C₉H₄O₄⁻, MS/MS fragments as reported [88].

Fig.3A .Structures of phenylethanoid/phenylpropanoid compounds in *L.ovalifolium* HasskFig 3B Structures of iridoid compounds in *L. ovalifolium* Hassk

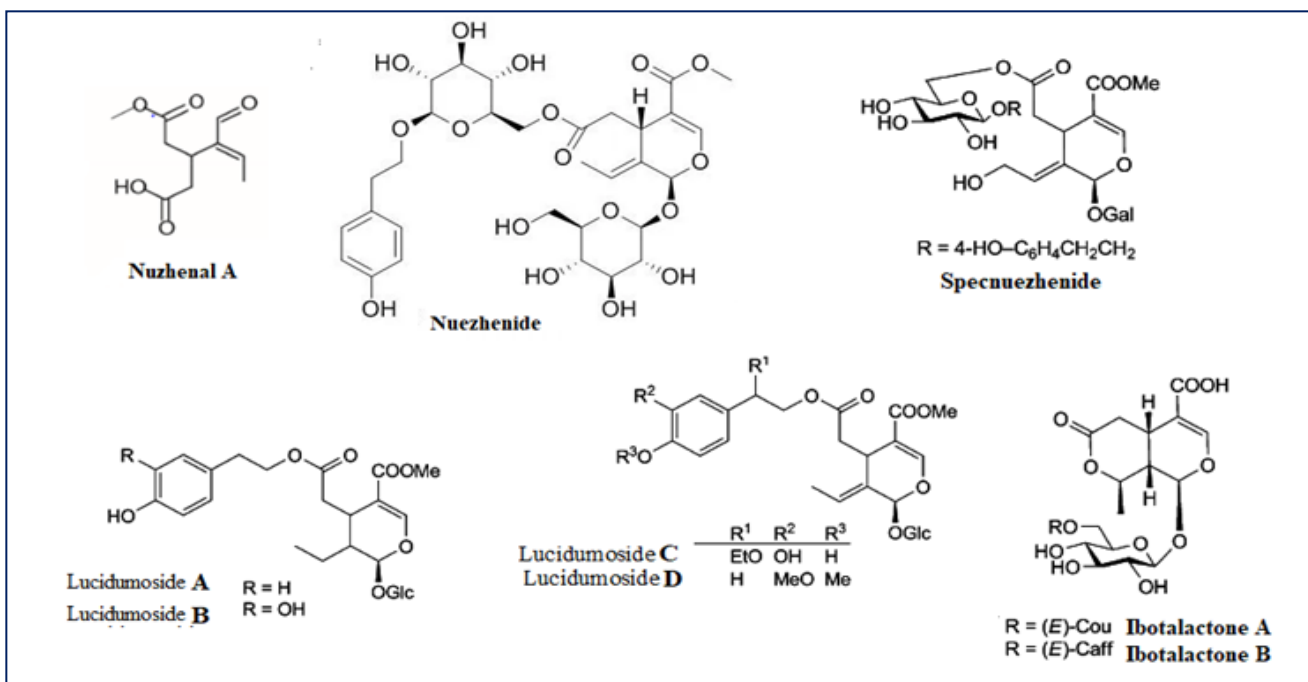
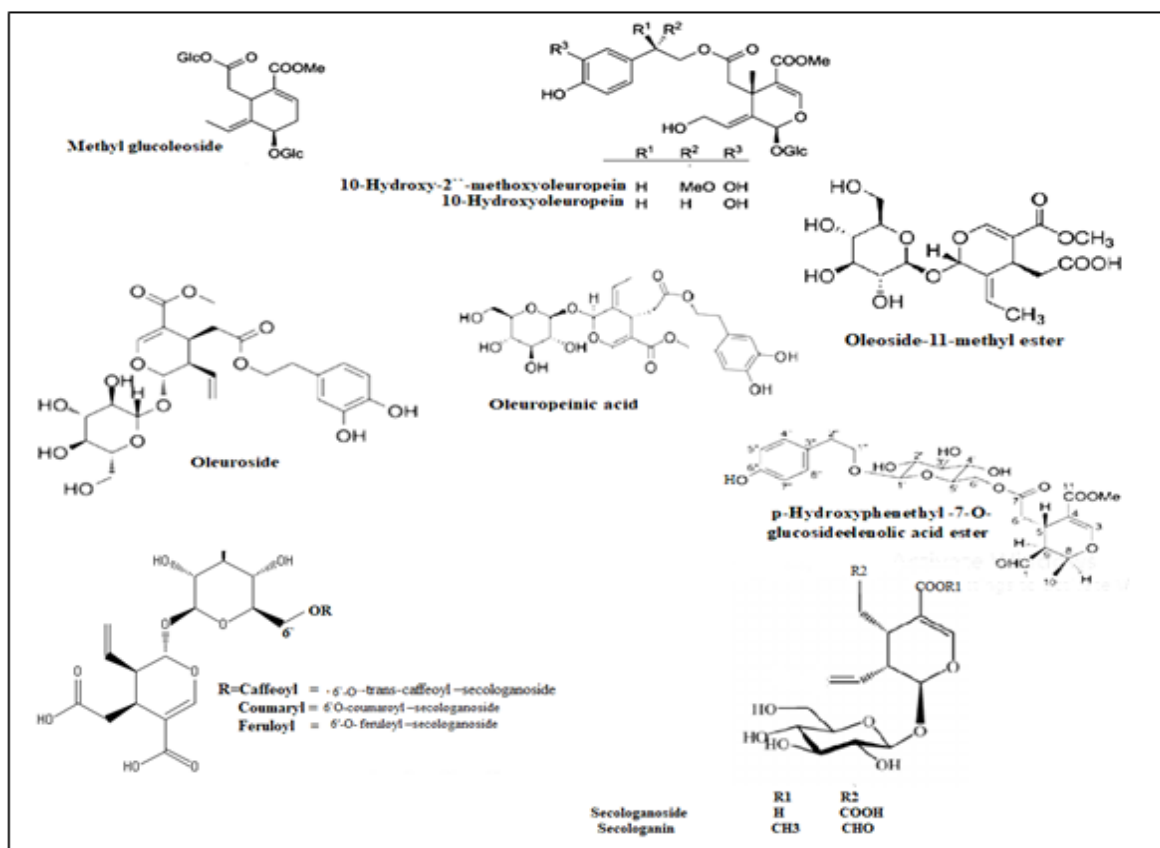
Fig 3C: Structures of iridoid compounds in *L. ovalifolium* HasskFig 3D: Structures of iridoid compounds in *L. ovalifolium* Hassk

Table 1: Metabolites detected via LC/MS/MS analysis of ethyl acetate fraction of *Ligustrum ovalifolium* Hassk aerial parts in negative ionization mode (Tentative identification).

Peak no	Rt	Compound class	Compounds	[M-H] ⁻	Molecular ion formula	MS/MS	Ref.
1	1.15	Phenolic acid	Vanillic acid	167.00	C ₈ H ₈ O ₄ ⁻	152, 137, 123, 108	[34]
2	1.41	Phenolic acid	Chlorogenic acid	352.96	C ₁₆ H ₁₇ O ₉ ⁻	191,173,135	[35]
3	1.55	Phenylethanoid	Hydroxytyrosol glucoside	315.00	C ₁₄ H ₁₉ O ₈ ⁻	153, 135, ,123	[42,43, 91]
4	1.56	Phenylethanoid	Hydroxytyrosol	153.02	C ₈ H ₉ O ₃ ⁻	123	
5	1.65	Ester of phenolic	Feruloyl quinic acid	367.00	C ₁₇ H ₁₉ O ₉ ⁻	193, 191, 173	[37]
6	1.70	Iridoid derivatives	<i>Trans</i> -caffeoyl – secologanoside	550.95	C ₂₅ H ₂₇ O ₁₄ ⁻	507, 393, 389, 323, 170	[68,69, 92]
7	1.8	Phenylethanoid	Tyrosol	137.00	C ₈ H ₉ O ₂ ⁻	119, 107	[93]
8	1.81	Phenolic acid	Caffeic acid	179.03	C ₉ H ₈ O ₄ ⁻	135	[36]
9	1.91	Phenylethanoid	Salidroside	299.02	C ₁₄ H ₁₉ O ₇ ⁻	179, 137, 119,	[93,45]
10	1.94	Phenolic acid	Coumaroylquinic acid	337.02	C ₁₆ H ₁₇ O ₈ ⁻	191, 163, 173	[37]
11	2.57	Secoiridoid derivatives	Coumaroyl – secologanoside	535.00	C ₂₅ H ₂₇ O ₁₃ ⁻	491, 389, 307, 163, 145	[68,69, 92]
12	2.83	Secoiridoid	Feruloyl –secologanoside	565.00	C ₂₆ H ₂₉ O ₁₄ ⁻	521, 389, 337, 193,	
13	3.44	Coumarin	Esculetin	177.00	C ₉ H ₆ O ₄ ⁻	149, 133, 121, 105	[88]
14	4.20	Secoiridoid	Ibotalactone B	550.99	C ₂₅ H ₂₇ O ₁₄ ⁻	507, 389, 323, 179,	[66]
15	4.28	Flavonoid (Flavonol-O-)	Quercetin -O-hexoside	462.93	C ₂₁ H ₁₉ O ₁₂ ⁻	301, 300, 271, 255,	[39]
16	4.32	Lignan	Olivil -O-glucoside	537.97	C ₂₆ H ₃₃ O ₁₂ ⁻	375, 345, 327, 195,	[94]
17	4.62	Iridoid	10-Hydroxyoleoside	433.00	C ₁₈ H ₂₅ O ₁₂ ⁻	389, 257, 225	[66]
18	4.87	Secoiridoid	Ligujaponoside B	571.00	C ₂₅ H ₃₂ O ₁₅ ⁻	539, 511, 359, 179, 151	[14]
19	5.24	Flavonoid (Flavonol-O-)	Rutin	609.92	C ₁₇ H ₂₉ O ₁₆ ⁻	463, 301	[39,95,
20	5.63	Secoiridoid	Ibotalactone A	535.00	C ₂₅ H ₂₇ O ₁₃ ⁻	491, 389, 307, 163, 145	[66]
21	5.89	Secoiridoid	Ligujaponoside A	555.00	C ₂₅ H ₃₁ O ₁₄ ⁻	523, 343, 179, 151	[14]
22	6.14	Secoiridoid	Methyl glucooleoside	564.95	C ₂₃ H ₃₃ O ₁₆ ⁻	403, 341, 295, 235, 193	[66]
23	6.51	Lignan	Olivil	375.01	C ₂₀ H ₂₃ O ₇ ⁻	359, 327, 195, 179, 165	[94]
24	6.54	Secoiridoid	Neonuezhenide	701.00	C ₃₁ H ₄₁ O ₁₈ ⁻	539, 469, 437, 315	[62]
25	6.59	Phenylpropanoid glycoside	Acteoside	622.98	C ₂₉ H ₃₅ O ₁₅ ⁻	461, 161	[94]
26	6.65	Flavonoids (Flavone-O-)	Kaempferol-O-hexoside	446.95	C ₂₁ H ₁₉ O ₁₁ ⁻	327, 285	[96]
27	6.74	Phenylethanoid glycoside	Ibotanolide B	477.00	C ₂₃ H ₂₅ O ₁₁ ⁻	315, 179, 161	[46]
28	6.78	Iridoid	10-Hydroxyoleuropein	555.00	C ₂₅ H ₃₁ O ₁₄ ⁻	523, 393, 307, 273	[64, 97]
29	6.84	Phenylpropanoid glycoside	Isoacteoside	622.98	C ₂₉ H ₃₆ O ₁₅ ⁻	461, 161	[94]
30	6.91	Secoiridoid	Nuzhenal A	213.12	C ₁₀ H ₁₃ O ₅ ⁻	183, 195, 177	[19]
31	6.92	Secoiridoid	(2 ^{''} R)-10-hydroxy-2 ^{''} -methoxyoleuropeins	585.00	C ₂₆ H ₃₃ O ₁₅ ⁻	553, 419, 401, 387, 337, 303, 151	[60]
32	6.99	Secoiridoid	Nuezhenide	685.02	C ₃₁ H ₄₁ O ₁₇ ⁻	555, 523, 453, 421, 299, 223, 179	[69,97]
33	7.01	Phenylpropanoid glycoside	Ligupurpurososide A	769.00	C ₃₅ H ₄₅ O ₁₉ ⁻	607, 301, 161, 133	[39]
34	7.04	Secoiridoid	ligustaloside A	554.94	C ₂₅ H ₃₁ O ₁₄ ⁻	523, 393, 307, 273	[42,39]
35	7.12	Flavonoids (Flavone-O-)	Rhoifolin (apigenin 7-O-neohesperidoside)	577.02	C ₂₇ H ₂₉ O ₁₄ ⁻	269, 431	[98]

Peak no	Rt	Compound class	Compounds	[M-H] ⁻	Molecular ion formula	MS/MS	Ref.
36	7.22	Secoiridoid	Specnuezhenide	685.00	C ₃₁ H ₄₁ O ₁₇ ⁻	555, 523, 453, 421, 299, 223, 179, 119	[99]
37	7.27	Lignan glucoside	Pinoresinol -O-glucoside	519.04	C ₂₆ H ₃₂ O ₁₁ ⁻	357, 151, 136	[100]
38	7.28	Secoiridoid	10-Hydroxy ligustroside	539.02	C ₂₅ H ₃₁ O ₁₃ ⁻	507, 377, 419, 401, 291, 275	
39	7.34	Secoiridoid glucosides	p-Hydroxyphenethyl -7-O-glucosideelenolic acid ester	523.00	C ₂₅ H ₃₁ H ₁₂	453, 431, 421, 387, 269, 223	[67]
40	7.38	Flavonoids (Flavone-O)	Apigenin 7-O-hexoside	431.00	C ₂₁ H ₁₉ O ₁₀ ⁻	269, 268	[42]
41	7.39	Flavonoids (Flavone-O)	Isorhoifolin (Apigenin-7-O-rutinoside)	577.00	C ₂₇ H ₂₉ O ₁₄ ⁻	431, 269	[98,63]
42	7.41	Lignan	Pinoresinol	357.02	C ₂₀ H ₂₂ O ₆	151, 136	[94]
43	7.47	Secoiridoid	Isonuezhenide	685.12	C ₃₁ H ₄₁ O ₁₇ ⁻	523, 453, 421, 299, 223, 179	[63]
44	7.51	Secoiridoid	Ligustaloid B	539.03	C ₂₅ H ₃₁ O ₁₃ ⁻	377, 419, 291	[42, 39]
45	7.58	Lignan	Eucommin A	549.09	C ₂₇ H ₃₃ O ₁₂ ⁻	387, 372, 357, 181, 166, 151, 136	[94]
46	7.60	Secoiridoid	Lucidumoside D	567.02	C ₂₇ H ₃₅ O ₁₃ ⁻	521, 489, 359, 341, 303, 273, 251	[10, 64]
47	7.80	Secoiridoid	Oleoside-11-methylester	403.04	C ₁₇ H ₂₃ O ₁₁ ⁻	388, 373, 343, 328, 188, 139	[64,91, 101]
48	7.87	Secoiridoid derivatives	Ligustrohemiacetal B	377.03	C ₁₉ H ₂₁ O ₈ ⁻	359, 331, 291, 257, 137	[60,61]
49	7.92	Flavonoids (Flavone)	Luteolin	285.00	C ₁₅ H ₉ O ₆ ⁻	175, 151, 133	[41,10 2]
50	7.93	Phenolic acid	Ferulic acid	193.02	C ₁₀ H ₉ O ₄ ⁻	161, 133	[103]
51	8.11	Secoiridoid	Oleuropeinic acid	569.95	C ₂₅ H ₂₉ O ₁₅ ⁻	537, 305, 151, 123	[104, 105]
52	8.16	Secoiridoid	Lucidumoside B	541.01	C ₂₅ H ₃₃ O ₁₃ ⁻	403, 389, 379, 361, 221	[106,1 0.64]
53	8.17	Secoiridoid derivatives	ligustaloid A dimethyl acetal*	601.01	C ₂₇ H ₃₇ O ₁₅ ⁻	465, 439, 407, 308	[42,39]
54	8.22	Iridoid	Oleuropein*	539.01	C ₂₅ H ₃₁ O ₁₃ ⁻	403, 387, 377, 307, 275, 223	[64,91, 101]
55	8.74	Iridoid	Oleuroside	539.02	C ₂₅ H ₃₁ O ₁₃ ⁻	403, 387, 377, 307, 291, 275, 223	[108]
56	8.62	Lignan-O-glucoside	Syringaresinol O-glucoside	579.01	C ₂₈ H ₃₅ O ₁₃ ⁻	533, 387, 371, 356	[109]
57	8.70	Iridoid-O-glucoside	Oleoside/secologanoside	389.04	C ₁₆ H ₂₁ O ₁₁ ⁻	345(, 209, 165, 121	[68,69]
58	8.88	Secoiridoid	ligustaloid B dimethyl acetal*	585.05	C ₂₇ H ₃₇ O ₁₆ ⁻	423, 321, 291	[42,39]
59	9.01	Secoiridoid	Ligustroside*	523.17	C ₂₅ H ₃₁ O ₁₂ ⁻	361, 291, 259	[42,11 0,107.6]
60	9.01	Iridoid	Lucidumoside A	525.03	C ₂₅ H ₃₃ O ₁₂ ⁻	363, 293, 261, 259, 139	[10, 64]
61	9.15	Iridoid	Lucidumoside C	583.02	C ₂₇ H ₃₅ O ₁₄ ⁻	535, 505, 369, 357, 195, 165, 151	
62	9.21	Flavonoids (Flavone)	Apigenin	269.03	C ₁₅ H ₉ O ₅ ⁻	151, 149, 117	[41]
63	9.34	Iridoid	Neonuezhenide	701.01	C ₃₁ H ₄₁ O ₁₈ ⁻	669, 563, 539, 359, 291, 161	[62]
64	9.49	Flavonoids	Kaempferol-O-methyl ether	299.00	C ₁₆ H ₁₁ O ₆ ⁻	284, 256, 227, 151	[41,40]
65	9.58	Secoiridoid	Secologanin	387.04	C ₁₇ H ₂₃ O ₁₀ ⁻	357, 181, 151	[111]
66	15.4	Triterpenoid	2-Hydroxyoleanolic acid	471.18	C ₃₀ H ₄₇ O ₄ ⁻	427	[75]

Peak no	Rt	Compound class	Compounds	[M-H] ⁻	Molecular ion formula	MS/MS	Ref.
67	15.8	Triterpenoid	2-Hydroxyursolic acid	471.20	C ₃₀ H ₄₇ O ₄ ⁻	453, 407	[74]
68	17.61	Unsaturated fatty	Linolenic acid	277.13	C ₁₈ H ₂₉ O ₂ ⁻	277,259, 127	[112]
69	18.68	Secoiridoid	Liguluciridoids B	301.14	C ₁₄ H ₂₁ O ₇ ⁻	285, 217	
70	19.02	Unsaturated fatty	Hexadecenoic acid	253.14	C ₁₆ H ₂₉ O ₂ ⁻	207, 235	
71	19.39	Saturated fatty	Hexadecanoic acid	255.16	C ₁₆ H ₃₁ O ₂ ⁻	237	
72	20.20	Triterpenoids	Betulnic acid	455.22	C ₃₀ H ₄₇ O ₃ ⁻	438, 411, 393	[116]
73	20.40	Unsaturated fatty	Linoleic acid	279.16	C ₁₈ H ₃₁ O ₂ ⁻	279, 233, 193	[117]
74	20.92	Triterpenoids	Oleanolic acid	455.27	C ₃₀ H ₄₇ O ₃ ⁻	407	[106]
75	21.15	Triterpenoids	Ursolic acid	455.33	C ₃₀ H ₄₇ O ₃ ⁻	407	[116]
76	21.55	Triterpenoids	Erythrodiol	441.08	C ₃₀ H ₄₉ O ₂ ⁻	369	[118]
77	23.17	Unsaturated fatty	Oleic acid	281.16	C ₁₈ H ₃₃ O ₂ ⁻	281	[113]

*Metabolites previously reported in *L. ovalifolium* Hassk

4. Molecular docking

SARS CoV-2 virus was reported to possess a large single stranded RNA that encodes for a group of structural and non-structural proteins which are responsible for viral replication, survival and pathogenicity of the virus[89]. Among the structural proteins, spike protein (S) plays an important role in viral recognition and entry into host cell through binding of receptor binding domain (RBD) in the S1 subunit of viral spike protein to host angiotensin-converting enzyme 2 (hACE2) followed by fusion of S2 subunit to host cell membrane.

On the other hand, viral main protease (M^{Pro}) which is chymotrypsin-like protease is responsible for the cleavage of the two viral polyproteins pp1a and pp1b into several protein units which is an essential process for subsequent viral replication[90]. Awing to their crucial rule in viral replication and pathogenesis, both viral spike protein (S) and main protease (M^{Pro}) are considered as major targets for the discovery of antiviral agents against SARS Cov-2 virus. We have exploited the molecular docking study to reveal the possible underlying mechanism for the antiviral activity of the biologically active 90% methanol (fraction3) from *L. ovalifolium* crude extract.

The detected phytoconstituents by LC/MS/MS metabolic profiling from (fraction3) were docked against SARS Cov-2 main protease (M^{Pro}) and spike protein (S) while as their binding affinity and binding interactions toward these target proteins were assigned. (Table 2). Acteoside (25), (2`R)-10-hydroxy-2``-methoxyoleuropeins (31), ligustaloside A (34) and rutin (19) exhibited outstanding binding affinities toward the active site of M^{Pro} and achieved docking scores of -13.58, -11.93,

-11.92 and -11.22 kcal/mol, respectively which overtook the docking score achieved by the co-crystallized inhibitor (-10.73 kcal/mol).

The docking pose of the top scoring compound acetoside (**25**) revealed a similar binding mode to that of the co-crystallized inhibitor as it occupied the four subsites (S1', S1, S2 and S4) of the substrate binding pocket. The dihydroxy phenyl ring of the caffeoyl moiety was inserted in the S1' subsite and formed two hydrogen bonds with Thr26 while its carbonyl group along with the glucosyl moiety occupied S2 subsite and formed hydrogen bonds with Gln189 and Glu166 respectively. The rhamnosyl moiety extended toward S2 subsite forming hydrogen bond with Asn142 and the hydroxy tyrosolyl phenyl ring was incorporated in S4 subsite forming hydrogen bond with Gln189 and pi-alkyl interaction with Pro168. (**Figure 4**)

On the other hand, the best binding affinities against receptor binding domain (RBD) of SARS Cov-2 spike protein were exhibited by ligupurpurosides A (**33**), isoacetoside (**29**), ibotalactone B (**14**) and acetoside (**25**) which have achieved docking scores of -10.16, -8.97, -8.43 and -7.97 kcal/mol, respectively. Analysis of the best docking pose of the top scoring compound ligupurpurosides A (**33**) revealed that it has occupied a relatively large portion of the spike protein RBD- hACE2 binding interface forming several interactions with key residues which mediates the binding between RBD and hACE2.

Hydroxy tyrosolyl moiety formed three hydrogen bonds with Glu484 and Gln493, caffeoyl moiety formed one hydrogen bond with Glu406 and hydrophobic pi-cation interaction with Arg403, middle rhamnosyl formed three hydrogen bonds with Tyr453 and Ser494 while terminal rhamnosyl formed three hydrogen bonds with Gly496 and Gln 498 and hydrophobic pi-alkyl interaction with Tyr505. (**Fig 5**).

The abovementioned results suggest that the antiviral activity of 90% methanol fraction of *L. ovalifolium* Hassk against SARS-Cov2 could be attributed to the ability of several phytoconstituents to block the proteolytic activity of M^{Pro} or disrupt the interaction between viral spike protein with hACE2 receptor.

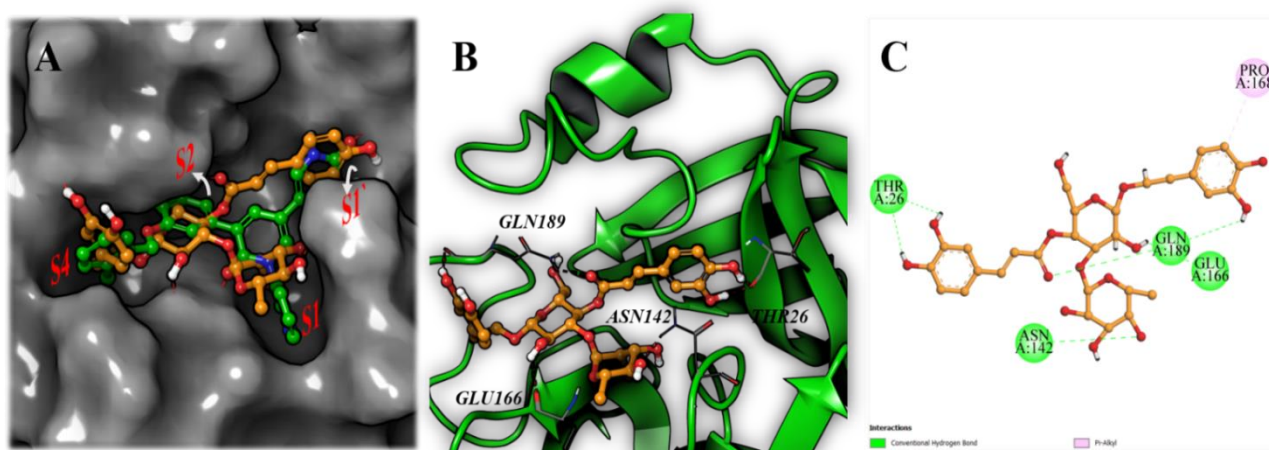


Figure 4. The docking pose of acetoside in the catalytic site of SARS Cov-2 M^{Pro} (PDB:7M8P). (A) Surface presentation illustrates the superposition of co-crystal inhibitor (green) and acetoside (orange) in the catalytic site. (B) cartoon presentation of the docking pose. (C) 2D presentation of binding interaction of acetoside with catalytic site residues

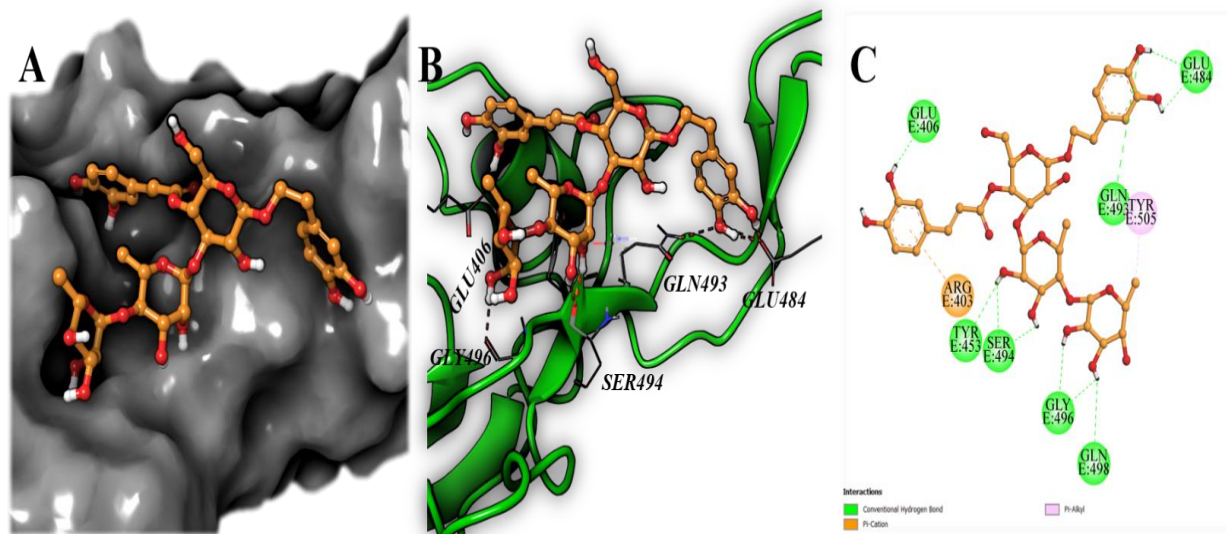


Figure 5. The docking pose of ligupurpuroside A in the RBD of SARS Cov-spike protein (PDB:6M0J). (A) Surface presentation (B) cartoon presentation (C) 2D presentation of binding interaction binding site residues

5. Conclusion

L. ovalifolium Hassk is an important plant belongs to family Oleaceae or olive family. Plants belongs to his family enriched with valuable constituents as iridoids, triterpenoids, phenylethanoid/phenylpropanoids and other compounds which had various biological activities as antioxidant, hepatoprotective, anti-inflammatory, antiviral and other biological activities. In our study LO aerial parts different extracts were screened for the first time as antiviral against SARS-Cov2 virus, the active extract was analyzed by LC/MS/MS which results in identification of 77 compounds the most abundant compounds were secoiridoids, triterpenoids, phenylethanoid/phenylpropanoid, lignin, flavonoids and other compounds, some compounds from each class were docked against SARS Cov-2 main protease (M^{Pro}) and spike protein (S). it was found that acteoside, (2`R)-10-hydroxy-2`-methoxyoleuropeins, ligustaloside A and rutin exhibited outstanding binding affinities toward the active site of M^{Pro} while the best binding affinities against receptor binding domain (RBD) of SARS Cov-2 spike protein were exhibited by ligupurpuroside A, isoacteoside, ibotalactone B and acteoside. These important finding suggest the possible use of the active fraction of LO as antiviral against SARS Cov-2.

6. Conflicts of interest

There are no conflicts to declare.

7. Formatting of funding sources

No – funding stated.

8. References

1. Britannica, The Editors of Encyclopaedia. "Oleaceae". *Encyclopedia Britannica*, 16 Mar.2009, <https://www.britannica.com/plant/Oleaceae>. Accessed 21 April 2024

2. Jensen, S. R., Franzyk, H., & Wallander, E. (2002). Chemotaxonomy of the Oleaceae: iridoids as taxonomic markers. *Phytochemistry*, 60(3), 213-231.
3. Harsha, M., Ashish, M., Pranav, V., Megha, J., & Chokotia, L. S. (2013). Review on pharmacological activities of *Ligustrum ovalifolium*. *International Journal of Research and Development in Pharmacy and Life Sciences*, 2(4), 474-477.
4. Ćurčić, M.G., Stanković, M.S., Mrkalić, E.M., Matović, Z.D., Banković, D.D., Cvetković, D.M., Đačić, D.S. and Marković, S.D. (2012). Antiproliferative and proapoptotic activities of methanolic extracts from *Ligustrum vulgare* L. as an individual treatment and in combination with palladium complex. *International Journal of Molecular Sciences*, 13(2), 2521-2534.
5. Gao, D., Li, Q., Li, Y., Liu, Z., Fan, Y., Liu, Z., Zhao, H., Li, J. and Han, Z. (2009). Antidiabetic and antioxidant effects of oleanolic acid from *Ligustrum lucidum* Ait in alloxan-induced diabetic rats. *Phytotherapy Research: An International Journal Devoted to Pharmacological and Toxicological Evaluation of Natural Product Derivatives*, 23(9), 1257-1262.
6. Lin, H. M., Yen, F. L., Ng, L. T., & Lin, C. C. (2007). Protective effects of *Ligustrum lucidum* fruit extract on acute butylated hydroxytoluene-induced oxidative stress in rats. *Journal of Ethnopharmacology*, 111(1), 129-136.
7. Wu, C. R., Lin, W. H., Hseu, Y. C., Lien, J. C., Lin, Y. T., Kuo, T. P., & Ching, H. (2011). Evaluation of the antioxidant activity of five endemic *Ligustrum* species leaves from Taiwan flora in vitro. *Food chemistry*, 127(2), 564-571.
8. Zhu, F., Cai, Y. Z., Sun, M., Ke, J., Lu, D., & Corke, H. (2009). Comparison of major phenolic constituents and in vitro antioxidant activity of diverse Kudingcha genotypes from *Ilex kudingcha*, *Ilex cornuta*, and *Ligustrum robustum*. *Journal of Agricultural and Food Chemistry*, 57(14), 6082-6089.
9. Fan, L., Liao, C.H., Li, S.G., Huang, X.J., Hu, X.P., Song, X., Fan, C.L., Wang, Y., Ye, W.C., Kang, Q.R. and Zheng, K. (2015). Phenylethanoid and secoiridoid glycosides from the leaves of *Ligustrum purpurascens*. *Phytochemistry letters*, 13, 177-181.
10. He, Z. D., But, P. P. H., Chan, T. W. D., DONG, H., XU, H. X., LAU, C. P., & Sun, H. D. (2001). Antioxidative glucosides from the fruits of *Ligustrum lucidum*. *Chemical and Pharmaceutical Bulletin*, 49(6), 780-784.
11. Pérez, J. A., Hernández, J. M., Trujillo, J. M., & López, H. (2005). Iridoids and secoiridoids from Oleaceae. *Studies in natural products chemistry*, 32, 303-363.
12. Pieroni, A., Pachaly, P., Huang, Y., Van Poel, B., & Vlietinck, A. J. (2000). Studies on anti-complementary activity of extracts and isolated flavones from *Ligustrum vulgare* and *Phillyrea latifolia* leaves (Oleaceae). *Journal of ethnopharmacology*, 70(3), 213-217.
13. Xu, X. H., Yang, N. Y., Qian, S. H., Xie, N. I. N. G., & Duan, J. A. (2008). Dammarane triterpenes from *Ligustrum lucidum*. *Journal of Asian natural products research*, 10(1), 33-37.
14. Ngo, Q. M. T., Lee, H. S., Kim, J. A., Woo, M. H., & Min, B. S. (2017). Chemical constituents from the fruits of *Ligustrum japonicum* and their inhibitory effects on T cell activation. *Phytochemistry*, 141, 147-155.
15. Cheng, M., Wang, Q., Fan, Y., Liu, X., Wang, L., Xie, R., Ho, C.C. and Sun, W. (2011). A traditional Chinese herbal preparation, Er-Zhi-Wan, prevent ovariectomy-induced osteoporosis in rats. *Journal of ethnopharmacology*, 138(2), 279-285.
16. Shoemaker, M., Hamilton, B., Dairkee, S. H., Cohen, I., & Campbell, M. J. (2005). In vitro anticancer activity of twelve Chinese medicinal herbs. *Phytotherapy Research: An International Journal Devoted to Pharmacological and Toxicological Evaluation of Natural Product Derivatives*, 19(7), 649-651.

17. Yim, T. K., Wu, W. K., Pak, W. F., & Ko, K. M. (2001). Hepatoprotective action of an oleanolic acid-enriched extract of *Ligustrum lucidum* fruits is mediated through an enhancement on hepatic glutathione regeneration capacity in mice. *Phytotherapy Research*, 15(7), 589-592.
18. Xu, X. H., Yang, N. Y., Qian, S. H., Xie, N., Yu, M. Y., & Duan, J. A. (2007). Study on flavonoids in *Ligustrum lucidum*. *Journal of Chinese Medicinal Materials*, 30(5), 538-540.
19. Aoki, S., Honda, Y., Kikuchi, T., Miura, T., Sugawara, R., Yaoita, Y., Kikuchi, M. and Machida, K. (2012). Six new secoiridoids from the dried fruits of *Ligustrum lucidum*. *Chemical and Pharmaceutical Bulletin*, 60(2), 251-256.
20. Zhang, Y., Leung, P. C., Che, C. T., Chow, H. K., Wu, C. F., & Wong, M. S. (2008). Improvement of bone properties and enhancement of mineralization by ethanol extract of *Fructus Ligustri Lucidi*. *British journal of nutrition*, 99(3), 494-502.
21. Ko, C. H., Siu, W. S., Lau, C. P., Lau, C. S., Fung, K. P., & Leung, P. C. (2010). Osteoprotective effects of *Fructus Ligustri Lucidi* aqueous extract in aged ovariectomized rats. *Chinese Medicine*, 5, 1-9.
22. Li, G., Zhang, X.A., Zhang, J.F., Chan, C.Y., Yew, D.T.W., He, M.L., Lin, M.C.M., Leung, P.C. and Kung, H.F. (2010). Ethanol extract of *Fructus Ligustri Lucidi* promotes osteogenesis of mesenchymal stem cells. *Phytotherapy Research: An International Journal Devoted to Pharmacological and Toxicological Evaluation of Natural Product Derivatives*, 24(4), 571-576.
23. Dong, X. L., Zhao, M., Wong, K. K., Che, C. T., & Wong, M. S. (2012). Improvement of calcium balance by *Fructus Ligustri Lucidi* extract in mature female rats was associated with the induction of serum parathyroid hormone levels. *British Journal of Nutrition*, 108(1), 92-101.
24. Moldovan, B., Sincari, V., Perde-Schrepler, M., & David, L. (2018). Biosynthesis of silver nanoparticles using *Ligustrum ovalifolium* fruits and their cytotoxic effects. *Nanomaterials*, 8(8), 627.
25. Machida, K., Yamaguchi, T., Kamiya, Y., & Kikuchi, M. (1997). Acylated triterpenoids from *Ligustrum ovalifolium*. *Phytochemistry*, 46(5), 977-979.
26. Hosny, M., Ragab, E. A., Mohammed, A. E. S. I., & Shaheen, U. Y. (2009). New secoiridoids from *Ligustrum ovalifolium* and their hypotensive activity. *Pharmacognosy Research*, 1(2).
27. Rawah H. Elkousy, Zeinab N. A. Said, Mohamed A. Ali, Omnia Kutkat and Salwa A. Abu El Wafa. Anti-SARS-CoV-2 in vitro potential of castor oil plant (*Ricinus communis*) leaf extract: in-silico virtual evidence 4, 2023 <https://doi.org/10.1515>
28. Mosmann, T. (1983). Rapid colorimetric assay for cellular growth and survival: application to proliferation and cytotoxicity assays. *Journal of immunological methods*, 65(1-2), 55-63.
29. Muhseen, Z. T., Hameed, A. R., Al-Hasani, H. M., ul Qamar, M. T., & Li, G. (2020). Promising terpenes as SARS-CoV-2 spike receptor-binding domain (RBD) attachment inhibitors to the human ACE2 receptor: Integrated computational approach. *Journal of molecular liquids*, 320, 114493.
30. Sayed, D. F., Afifi, A. H., Temraz, A., & Ahmed, A. H. (2023). Metabolic Profiling of *Mimusops elengi* Linn. Leaves extract and in silico anti-inflammatory assessment targeting NLRP3 inflammasome. *Arabian Journal of Chemistry*, 16(6), 104753.
31. Wang, Z. H., Hsu, C. C., & Yin, M. C. (2009). Antioxidative characteristics of aqueous and ethanol extracts of glossy privet fruit. *Food Chemistry*, 112(4), 914-918.

32. Huang, Y. L., Oppong, M. B., Guo, Y., Wang, L. Z., Fang, S. M., Deng, Y. R., & Gao, X. M. (2019). The Oleaceae family: A source of secoiridoids with multiple biological activities. *Fitoterapia*, *136*, 104155.
33. Wishart, D.S., Feunang, Y.D., Marcu, A., Guo, A.C., Liang, K., Vázquez-Fresno, R., Sajed, T., Johnson, D., Li, C., Karu, N. and Sayeeda, Z. (2018). HMDB 4.0: the human metabolome database for 2018. *Nucleic acids research*, *46*(D1), D608-D617.
34. Horai, H., Arita, M., Kanaya, S., Nihei, Y., Ikeda, T., Suwa, K., Ojima, Y., Tanaka, K., Tanaka, S., Aoshima, K. and Oda, Y. (2010). MassBank: a public repository for sharing mass spectral data for life sciences. *Journal of mass spectrometry*, *45*(7), 703-714.
35. Naveed, M., Hejazi, V., Abbas, M., Kamboh, A.A., Khan, G.J., Shumzaid, M., Ahmad, F., Babazadeh, D., FangFang, X., Modarresi-Ghazani, F. WenHua, L. and XiaoHui Z (2018). Chlorogenic acid (CGA): A pharmacological review and call for further research. *Biomedicine & pharmacotherapy*, *97*, 67-74.
36. Mata, A., Ferreira, J. P., Semedo, C., Serra, T., Duarte, C. M. M., & Bronze, M. R. (2016). Contribution to the characterization of *Opuntia* spp. juices by LC–DAD–ESI-MS/MS. *Food Chemistry*, *210*, 558-565.
37. Clifford, M. N., Zheng, W., & Kuhnert, N. (2006). Profiling the chlorogenic acids of aster by HPLC–MSn. *Phytochemical Analysis: An International Journal of Plant Chemical and Biochemical Techniques*, *17*(6), 384-393.
38. Cuyckens F, Claeys M (2004) Mass spectrometry in the structural analysis of flavonoids. *J Mass Spectrom* *JMS* *39*:1–15. <https://doi.org/10.1002/jms.585>
39. Ling, Z., Zeng, R., Zhou, X., Chen, F., Fan, Q., Sun, D., Chen, X., Wei, M., Wu, R. and Luo, W. (2022). Component analysis using UPLC-Q-Exactive Orbitrap-HRMS and quality control of Kudingcha (*Ligustrum robustum* (Roxb.) Blume). *Food Research International*, *162*, 111937.
40. Chernonosov, A. A., Karpova, E. A., & Lyakh, E. M. (2017). Identification of phenolic compounds in *Myricaria bracteata* leaves by high-performance liquid chromatography with a diode array detector and liquid chromatography with tandem mass spectrometry. *Revista Brasileira de Farmacognosia*, *27*, 576-579.
41. Jia, L., Fu, L., Wang, X., Yang, W., Wang, H., Zuo, T., Zhang, C., Hu, Y., Gao, X. and Han, L. (2018). Systematic profiling of the multicomponents and authentication of Erzhi Pill by UHPLC/Q-Orbitrap-MS oriented rapid polarity-switching data-dependent acquisition and selective monitoring of the chemical markers deduced from fingerprint analysis. *Molecules*, *23*(12), 3143.
42. Zhang, Y., He, Y., Liu, C., Liu, C., & Li, S. (2018). Screening and isolation of potential neuraminidase inhibitors from leaves of *Ligustrum lucidum* Ait. based on ultrafiltration, LC/MS, and online extraction-separation methods. *Journal of Chromatography B*, *1083*, 102-109.
43. Liu, X. F., Liang, J. Y., Sun, J. B., & Huang, X. F. (2018). Research progress of the Fructus *Ligustri lucidi* on the chemical compounds and pharmacological activity. *Strait Pharm. J*, *30*, 1-8.
44. Lu, S. H., Zuo, H. J., Huang, J., Chen, R., Pan, J. P., & Li, X. X. (2022). Phenylethanoid and phenylmethanoid glycosides from the leaves of *Ligustrum robustum* and their bioactivities. *Molecules*, *27*(21), 7390.
45. Ding, Y., Ju, Z., & Ma, C. (2018). A validated LC–MS/MS method for the determination of specnuezhenide and salidroside in rat plasma and its application to a pharmacokinetic study. *Biomedical Chromatography*, *32*(12), e4353.

46. Gao, M., Xue, X., Zhang, X., Chang, Y., Zhang, Q., Li, X., Wang, Y., Zhang, L., Li, Z., Dong, H. and Wang, W. (2022). Discovery of potential active ingredients of Er-Zhi-Wan, a famous traditional Chinese formulation, in model rat serum for treating osteoporosis with kidney-yin deficiency by UPLC-Q/TOF-MS and molecular docking. *Journal of Chromatography B*, 1208, 123397.
47. Su, D., Li, W., Xu, Q., Liu, Y., Song, Y., & Feng, Y. (2016). New metabolites of acteoside identified by ultra-performance liquid chromatography/quadrupole-time-of-flight MSE in rat plasma, urine, and feces. *Fitoterapia*, 112, 45-55.
48. Li, Y., Gan, L., Li, G. Q., Deng, L., Zhang, X., & Deng, Y. (2014). Pharmacokinetics of plantamajoside and acteoside from *Plantago asiatica* in rats by liquid chromatography–mass spectrometry. *Journal of pharmaceutical and biomedical analysis*, 89, 251-256.
49. Yang, Y., Xi, D., Wu, Y., & Liu, T. (2023b). Complete biosynthesis of the phenylethanoid glycoside verbascoside. *Plant Communications*, 4(4).
50. Xiao, Y., Ren, Q., & Wu, L. (2022). The pharmacokinetic property and pharmacological activity of acteoside: A review. *Biomedicine & pharmacotherapy*, 153, 113296.
51. Dinda, B. (2019). *Pharmacology and applications of naturally occurring iridoids*. Berlin/Heidelberg, Germany: Springer International Publishing.
52. Bianco, A. (1994). Recent developments in iridoids chemistry. *Pure and applied chemistry*, 66(10-11), 2335-2338.
53. Zheng, L. S., Liu, X. Q. (2009). Research progress of iridoids. *Res. Dev. Nat. Prod*, 21, 702–711.
54. Li, C. M., Luo, Y. W., & Tian, B. Y. (2015). Research progress on mass spectral fragmentation of iridoids. *J. Hebei Normal Univ*, 39, 522-526.
55. Pei, Y. H., Lou, H.X. (2016). *Natural Medicinal Chemistry*. People's Health Publishing House; Beijing, China, 192–195.
56. Ren, Z. J., Zhang, L. M., & He, K. Z. (2005). Extraction technology and pharmacological research progress of main components of *Gardenia jasminoides* Ellis. *Res. Dev. Nat. Prod*, 17, 831-836.
57. Picerno, P., Autore, G., Marzocco, S., Meloni, M., Sanogo, R., & Aquino, R. P. (2005). Anti-inflammatory activity of verminoside from *kigelia africana* and evaluation of cutaneous irritation in cell cultures and reconstituted human epidermis. *Journal of Natural Products*, 68(11), 1610-1614.
58. Akihisa, T., Matsumoto, K., Tokuda, H., Yasukawa, K., Seino, K.I., Nakamoto, K., Kuninaga, H., Suzuki, T. and Kimura, Y. (2007). Anti-inflammatory and potential cancer chemopreventive constituents of the fruits of *Morinda citrifolia* (Noni). *Journal of natural products*, 70(5), 754-757.
59. Zhang, Y., Mukwaya, E., Pan, H., Li, X. M., Yang, J. L., Ge, J., & Wang, H. Y. (2015a). Combination therapy of Chinese herbal medicine *Fructus Ligustri Lucidi* with high calcium diet on calcium imbalance induced by ovariectomy in mice. *Pharmaceutical Biology*, 53(7), 1082-1085.
60. Tanahashi, T., Takenaka, Y., Okazaki, N., Koge, M., Nagakura, N., & Nishi, T. (2009). Secoiridoid glucosides and unusual recycled secoiridoid aglycones from *Ligustrum vulgare*. *Phytochemistry*, 70(17-18), 2072-2077.
61. Pang, X., Zhao, J.Y., Yu, H.Y., Yu, L.Y., Wang, T., Zhang, Y., Gao, X.M. and Han, L.F. (2018). Secoiridoid analogues from the fruits of *Ligustrum lucidum* and their inhibitory activities against influenza A virus. *Bioorganic & Medicinal Chemistry Letters*, 28(9), 1516-1519.

62. Tóth, G., Barabás, C., Tóth, A., Kéry, Á., Béni, S., Boldizsár, I., Varga, E. and Noszál, B. (2016). Characterization of antioxidant phenolics in *Syringa vulgaris* L. flowers and fruits by HPLC-DAD-ESI-MS. *Biomedical chromatography*, 30(6), 923-932.
63. Li, H., Yao, W., Liu, Q., Xu, J., Bao, B., Shan, M., Cao, Y., Cheng, F., Ding, A. and Zhang, L. (2017). Application of UHPLC-ESI-Q-TOF-MS to identify multiple constituents in processed products of the herbal medicine *Ligustri Lucidi Fructus*. *Molecules*, 22(5), 689.
64. Quirantes-Piné, R., Lozano-Sánchez, J., Herrero, M., Ibáñez, E., Segura-Carretero, A., & Fernández-Gutiérrez, A. (2013). HPLC-ESI-QTOF-MS as a powerful analytical tool for characterising phenolic compounds in olive-leaf extracts. *Phytochemical Analysis*, 24(3), 213-223.
65. Bermúdez-Oria, A., Castejón, M. L., Rubio-Senent, F., Fernández-Prior, Á., Rodríguez-Gutiérrez, G., & Fernández-Bolaños, J. (2024). Isolation and structural determination of cis- and trans-p-coumaroyl-secologanoside (comselogoside) from olive oil waste (alperujo). Photoisomerization with ultraviolet irradiation and antioxidant activities. *Food chemistry*, 432, 137233.
66. Gao, B. B., She, G. M., & She, D. M. (2013). Chemical constituents and biological activities of plants from the genus *Ligustrum*. *Chemistry & Biodiversity*, 10(1), 96-128.
67. Yang, N. Y., Xu, X. H., Ren, D. C., Duan, J. A., Xie, N., Tian, L. J., & Qian, S. H. (2010). Secoiridoid constituents from the fruits of *Ligustrum lucidum*. *Helvetica Chimica Acta*, 93(1), 65-71.
68. Jerman Klen, T., Golc Wondra, A., Vrhovsek, U., & Mozetič Vodopivec, B. (2015). Phenolic profiling of olives and olive oil process-derived matrices using UPLC-DAD-ESI-QTOF-HRMS analysis. *Journal of Agricultural and Food Chemistry*, 63(15), 3859-3872.
69. Fu, S., Arráez-Roman, D., Segura-Carretero, A., Menéndez, J. A., Menéndez-Gutiérrez, M. P., Micol, V., & Fernández-Gutiérrez, A. (2010). Qualitative screening of phenolic compounds in olive leaf extracts by hyphenated liquid chromatography and preliminary evaluation of cytotoxic activity against human breast cancer cells. *Analytical and bioanalytical chemistry*, 397, 643-654.
70. Zhao, X., & Liu, J. (2020). Chemical Constituents From the Fruits of *Ligustrum lucidum* WT Aiton and Their Role on the Medicinal Treatment. *Natural Product Communications*, 15(4), 1934578X20922338.
71. Ma, S.C., He, Z.D., Deng, X.L., But, P.P.H., Ooi, V.E.C., Xu, H.X., Lee, S.H.S. and Lee, S.F. (2001). In vitro evaluation of secoiridoid glucosides from the fruits of *Ligustrum lucidum* as antiviral agents. *Chemical and pharmaceutical bulletin*, 49(11), 1471-1473.
72. Chen, Q., Zhang, Y., Zhang, W., & Chen, Z. (2011). Identification and quantification of oleanolic acid and ursolic acid in Chinese herbs by liquid chromatography-ion trap mass spectrometry. *Biomedical Chromatography*, 25(12), 1381-1388.
73. Ghiulai, R., Mioc, M., Racoviceanu, R., Prodea, A., Milan, A., Coricovac, D., Dehelean, C., Avram, Ș., Zamfir, A.D., Munteanu, C.V. and Ivan, V. (2022). Structural Investigation of Betulinic Acid Plasma Metabolites by Tandem Mass Spectrometry. *Molecules*, 27(21), 7359.
74. Gao, L., Li, C., Wang, Z., Liu, X., You, Y., Wei, H., & Guo, T. (2015). *Ligustri Lucidi Fructus* as a traditional Chinese medicine: A review of its phytochemistry and pharmacology. *Natural product research*, 29(6), 493-510.
75. Zhang, T., Dai, Y., & Yao, X. S. (2011). Chemical constituents of *Ligustrum lucidum*. *China Pharmacy*, 23, 2931-2932.

76. Zhang, Y., Zhang, C., Ren, R., & Liu, R. (2012). Simultaneous determination of seven major triterpenoids in *Pyrola decorata* H. Andres by LC-MS method. *Die Pharmazie-An International Journal of Pharmaceutical Sciences*, 67(10), 822-826.
77. Shen, P., Wang, W., Xu, S., Du, Z., Wang, W., Yu, B., & Zhang, J. (2020). Biotransformation of erythrodiol for new food supplements with anti-inflammatory properties. *Journal of agricultural and food chemistry*, 68(21), 5910-5916.
78. Cao, S., Wastney, M. E., Lachcik, P. J., Xiao, H. H., Weaver, C. M., & Wong, M. S. (2018). Both oleanolic acid and a mixture of oleanolic and ursolic acids mimic the effects of fructus *ligustri lucidi* on bone properties and circulating 1, 25-dihydroxycholecalciferol in ovariectomized rats. *The Journal of Nutrition*, 148(12), 1895-1902.
79. Sha, N. N., Zhao, Y. J., Zhao, D. F., Mok, D. K. W., Shi, Q., Wang, Y. J., & Zhang, Y. (2017). Effect of the water fraction isolated from *Fructus Ligustri Lucidi* extract on bone metabolism via antagonizing a calcium-sensing receptor in experimental type 1 diabetic rats. *Food & function*, 8(12), 4703-4712.
80. Sun, R. N., Guo, Y. L., Wang, J., Kong, L. B. (2013). Main active components of *Ligustrum lucidum* extract and their activity to inhibit hepatitis C virus replication. *Chin J Biochem Mol Biol*, 29(10), 956-961.
81. Yuan, Y., Shen, L. X., Pan, Y. (2019). Effect and mechanism of *Ligustrum lucidum* on pancreatic islet β cells in type 2 diabetic rats. *Chin J Tradit Chin Med*, 37(1), 208-210.
82. Gao, F. J. (2011). Extract of *Ligustri Lucidi Fructus* inhibits expression of angiogenic factors in human hepatocellular carcinoma cells. *Chin J Exp Tradit Med Formulae*, 17, 139-142.
83. Hu, B., Du, Q., Deng, S., An, H.M., Pan, C.F., Shen, K.P., Xu, L., Wei, M.M. and Wang, S.S. (2014). *Ligustrum lucidum* Ait. fruit extract induces apoptosis and cell senescence in human hepatocellular carcinoma cells through upregulation of p21. *Oncology Reports*, 32(3), 1037-1042.
84. Fiorentino, A., Ricci, A., D'Abrosca, B., Pacifico, S., Golino, A., Letizia, M., Piccolella, S. and Monaco, P. (2008). Potential food additives from *Carex distachya* roots: identification and in vitro antioxidant properties. *Journal of Agricultural and Food Chemistry*, 56(17), 8218-8225.
85. Hanhineva, K., Rogachev, I., Aura, A. M., Aharoni, A., Poutanen, K., & Mykkänen, H. (2012). Identification of novel lignans in the whole grain rye bran by non-targeted LC-MS metabolite profiling. *Metabolomics*, 8, 399-409.
86. Peterson, J., Dwyer, J., Adlercreutz, H., Scalbert, A., Jacques, P., & McCullough, M. L. (2010). Dietary lignans: physiology and potential for cardiovascular disease risk reduction. *Nutrition reviews*, 68(10), 571-603.
87. Yu, J., Kwon, H., Cho, E., Kang, R.H., Youn, K., Jun, M., Lee, Y.C., Ryu, J.H. and Kim, D.H. (2019). The effects of pinoreosinol on cholinergic dysfunction-induced memory impairments and synaptic plasticity in mice. *Food and chemical toxicology*, 125, 376-382.
88. Li, Y.Y., Song, Y.Y., Liu, C.H., Huang, X.T., Zheng, X., Li, N., Xu, M.L., Mi, S.Q. and Wang, N.S. (2012). Simultaneous determination of esculin and its metabolite esculetin in rat plasma by LC-ESI-MS/MS and its application in pharmacokinetic study. *Journal of chromatography B*, 907, 27-33.88.
89. Yadav, R., Chaudhary, J.K., Jain, N., Chaudhary, P.K., Khanra, S., Dhamija, P., Sharma, A., Kumar, A. and Handu, S. (2021). Role of structural and non-structural proteins and therapeutic targets of SARS-CoV-2 for COVID-19. *Cells*, 10(4), 821.

90. Kushwaha, P. P., Singh, A. K., Bansal, T., Yadav, A., Prajapati, K. S., Shuaib, M., & Kumar, S. (2021). Identification of natural inhibitors against SARS-CoV-2 drugable targets using molecular docking, molecular dynamics simulation, and MM-PBSA approach. *Frontiers in Cellular and Infection Microbiology*, *11*, 730288.
91. Peralbo-Molina, A., Priego-Capote, F., & Luque de Castro, M. D. (2012). Tentative identification of phenolic compounds in olive pomace extracts using liquid chromatography–tandem mass spectrometry with a quadrupole–quadrupole-time-of-flight mass detector. *Journal of Agricultural and Food Chemistry*, *60*(46), 11542-11550.
92. Sun, H., Liu, M., Lin, Z., Jiang, H., Niu, Y., Wang, H., & Chen, S. (2015). Comprehensive identification of 125 multifarious constituents in Shuang–huang–lian powder injection by HPLC-DAD-ESI-IT-TOF-MS. *Journal of Pharmaceutical and Biomedical Analysis*, *115*, 86-106.
93. Ke, Z., Ting, L., Xing-Cheng, G., Li-Bo, C., Jun, L., Peng-Fei, T., Qing-Qing, S. and Yue-Lin, S. (2020). Online energy-resolved MS boosts the potential of LC-MS towards metabolite characterization of salidroside and tyrosol. *Analytical Methods*, *12*(42), 5120-5127.
94. Li, J., Wang, M., Wang, X., Sun, L., Zhao, C., & Zhao, M. (2020). Rapid characterization of the chemical constituents of Duzhong Jiangya tablet by HPLC coupled with Fourier transform ion cyclotron resonance mass spectrometry. *Journal of Separation Science*, *43*(24), 4434-4460.
95. Taamalli, A.; Arraez-Roman, D.; Ibanez, E.; Zarrouk, M.; Segura-Carretero, A.; Fernandez-Gutierrez, A. Optimization of microwave-assisted extraction for the characterization of olive leaf phenolic compounds by using HPLC-ESI-TOF-MS/IT-MS(2). *J. Agric. Food. Chem.* **2012**, *60*, 791–798.
96. Romani, A., Pinelli, P., Mulinacci, N., Vincieri, F. F., Gravano, E., & Tattini, M. (2000). HPLC analysis of flavonoids and secoiridoids in leaves of *Ligustrum vulgare* L. (Oleaceae). *Journal of Agricultural and Food Chemistry*, *48*(9), 4091-4096.
97. Tóth, G., Alberti, Á., Sólyomváry, A., Barabás, C., Boldizsár, I., & Noszál, B. (2015). Phenolic profiling of various olive bark-types and leaves: HPLC–ESI/MS study. *Industrial Crops and Products*, *67*, 432-438.
98. Brito, A., Ramirez, J. E., Areche, C., Sepúlveda, B., & Simirgiotis, M. J. (2014). HPLC-UV-MS profiles of phenolic compounds and antioxidant activity of fruits from three citrus species consumed in Northern Chile. *Molecules*, *19*(11), 17400-17421.
99. Di Donna, L., Mazzotti, F., Napoli, A., Salerno, R., Sajjad, A., & Sindona, G. (2007). Secondary metabolism of olive secoiridoids. New microcomponents detected in drupes by electrospray ionization and high-resolution tandem mass spectrometry. *Rapid Communications in Mass Spectrometry: An International Journal Devoted to the Rapid Dissemination of Up-to-the-Minute Research in Mass Spectrometry*, *21*(3), 273-278.
100. Liao, X., Hong, Y., & Chen, Z. (2021). Identification and quantification of the bioactive components in *Osmanthus fragrans* roots by HPLC-MS/MS. *Journal of Pharmaceutical Analysis*, *11*(3), 299-307.
101. Bianco, A., Buiarelli, F., Cartoni, G., Coccioli, F., Jasionowska, R., & Margherita, P. (2003). Analysis by liquid chromatography-tandem mass spectrometry of biophenolic compounds in olives and vegetation waters, Part I. *Journal of Separation Science*, *26*(5), 409-416.
102. Yang, M., Li, J., Zhao, C., Xiao, H., Fang, X., & Zheng, J. (2023a). LC-Q-TOF-MS/MS detection of food flavonoids: Principle, methodology, and applications. *Critical reviews in Food Science and Nutrition*, *63*(19), 3750-3770.

103. Santana, I., Castelo-Branco, V.N., Guimarães, B.M., de Oliveira Silva, L., Peixoto, V.O.D.S., Cabral, L.M.C., Freitas, S.P. and Torres, A.G. (2019). Hass avocado (*Persea americana* Mill.) oil enriched in phenolic compounds and tocopherols by expeller-pressing the unpeeled microwave dried fruit. *Food chemistry*, 286, 354-361.
104. Rubio-Senent, F., Lama-Munoz, A., Rodríguez-Gutiérrez, G., & Fernandez-Bolanos, J. (2013). Isolation and identification of phenolic glucosides from thermally treated olive oil byproducts. *Journal of agricultural and food chemistry*, 61(6), 1235-1248.
105. Guo, N., Yu, Y., Ablajan, K., Li, L., Fan, B., Peng, J., Yan, H., Ma, F. and Nie, Y. (2011). Seasonal variations in metabolite profiling of the fruits of *Ligustrum lucidum* Ait. *Rapid Communications in Mass Spectrometry*, 25(12), 1701-1714.
106. Pacifico, S., Bláha, P., Faramarzi, S., Fede, F., Michaličková, K., Piccolella, S., Ricciardi, V. and Manti, L. (2022). Differential radiomodulating action of *Olea europaea* L. cv. Caiazzana leaf extract on human normal and cancer cells: a joint chemical and radiobiological approach. *Antioxidants*, 11(8), 1603.
107. Savarese, M., De Marco, E., & Sacchi, R. (2007). Characterization of phenolic extracts from olives (*Olea europaea* cv. Pisciottana) by electrospray ionization mass spectrometry. *Food Chemistry*, 105(2), 761-770.
108. Gentile, L., & Uccella, N. A. (2014). Selected bioactives from callus cultures of olives (*Olea europaea* L. Var. Coratina) by LC-MS. *Food research international*, 55, 128-136.
109. Sanz, M., de Simón, B.F., Cadahía, E., Esteruelas, E., Muñoz, A.M., Hernández, T., Estrella, I. and Pinto, E. (2012). LC-DAD/ESI-MS/MS study of phenolic compounds in ash (*Fraxinus excelsior* L. and *F. americana* L.) heartwood. Effect of toasting intensity at cooperage. *Journal of Mass Spectrometry*, 47(7), 905-918.
110. García-Villalba, R., Carrasco-Pancorbo, A., Oliveras-Ferraro, C., Vázquez-Martín, A., Menéndez, J. A., Segura-Carretero, A., & Fernández-Gutiérrez, A. (2010). Characterization and quantification of phenolic compounds of extra-virgin olive oils with anticancer properties by a rapid and resolutive LC-ESI-TOF MS method. *Journal of Pharmaceutical and Biomedical Analysis*, 51(2), 416-429.
111. Cardoso, S. M., Guyot, S., Marnet, N., Lopes-da-Silva, J. A., Renard, C. M., & Coimbra, M. A. (2005). Characterization of phenolic extracts from olive pulp and olive pomace by electrospray mass spectrometry. *Journal of the Science of Food and Agriculture*, 85(1), 21-32.
112. Cowan, A. K., Wolstenholme, B. N. (2016) Avocado. *Encyclopedia of food and health*. Elsevier, Amsterdam, 294–300.
113. Waly, D. A., Zeid, A. H. A., Attia, H. N., Ahmed, K. A., El-Kashoury, E. S. A., El Halawany, A. M., & Mohammed, R. S. (2023). Comprehensive phytochemical characterization of *Persea americana* Mill. fruit via UPLC/HR-ESI-MS/MS and anti-arthritis evaluation using adjuvant-induced arthritis model. *Inflammopharmacology*, 31(6), 3243-3262.
114. Smith, D.G., Martinelli, R., Besra, G.S., Illarionov, P.A., Szatmari, I., Brazda, P., Allen, M.A., Xu, W., Wang, X., Nagy, L. and Dowell, R.D. (2019). Identification and characterization of a novel anti-inflammatory lipid isolated from *Mycobacterium vaccae*, a soil-derived bacterium with immunoregulatory and stress resilience properties. *Psychopharmacology*, 236, 1653-1670.
115. Yang, S. T., Wu, X., Rui, W., Guo, J., & Feng, Y. F. (2015). UPLC/Q-TOF-MS analysis for identification of hydrophilic phenolics and lipophilic diterpenoids from *Radix Salviae Miltiorrhizae*. *Acta Chromatographica*, 27(4), 711-728.
116. Sut, S., Zengin, G., Maggi, F., Malagoli, M., & Dall'Acqua, S. (2019). Triterpene acid and phenolics from ancient apples of Friuli Venezia Giulia as nutraceutical ingredients: LC-MS study and in vitro activities. *Molecules*, 24(6), 1109.

117. La Nasa, J., Degano, I., Brandolini, L., Modugno, F., & Bonaduce, I. (2018). A novel HPLC-ESI-Q-ToF approach for the determination of fatty acids and acylglycerols in food samples. *Analytica chimica acta*, *1013*, 98-109.

118. Kosyakov, D. S., Ul'Yanovskii, N. V., & Falev, D. I. (2014). Determination of triterpenoids from birch bark by liquid chromatography-tandem mass spectrometry. *Journal of analytical chemistry*, *69*, 1264-1269.

m mass spectrometry. *Journal of analytical chemistry*, *69*, 1264-1269.